

**Mitochondrial respiratory states and rates:
Building blocks of mitochondrial physiology
Part 1.**

http://www.mitoeagle.org/index.php/MitoEAGLE_preprint_2018-02-08

Preprint version 24 (2018-02-15)

MitoEAGLE Network

Corresponding author: Gnaiger E

Contributing co-authors

Acuna-Castroviejo D, Ahn B, Alves MG, Amati F, Aral C, Arandarčikaitė O, Åsander Frostner E, Bailey DM, Bastos Sant'Anna Silva AC, Battino M, Beard DA, Ben-Shachar D, Bishop D, Borutaitė V, Breton S, Brown GC, Brown RA, Buettner GR, Calabria E, Cardoso LHD, Carvalho E, Casado Pinna M, Cervinkova Z, Chang SC, Chen Q, Chicco AJ, Chinopoulos C, Coen PM, Collins JL, Crisóstomo L, Davis MS, Dias T, Distefano G, Doerrier C, Drahota Z, Duchen MR, Ehinger J, Elmer E, Endlicher R, Fell DA, Ferko M, Ferreira JCB, Filipovska A, Fisar Z, Fisher J, Garcia-Roves PM, Garcia-Souza LF, Genova ML, Gonzalo H, Goodpaster BH, Gorr TA, Grefte S, Han J, Harrison DK, Hellgren KT, Hernansanz P, Holland O, Hoppel CL, Houstek J, Hunger M, Iglesias-Gonzalez J, Irving BA, Iyer S, Jackson CB, Jadiya P, Jansen-Dürr P, Jespersen NR, Jha RK, Kaambre T, Kane DA, Kappler L, Karabatsiakos A, Keijer J, Keppner G, Komlodi T, Kopitar-Jerala N, Krako Jakovljevic N, Kuang J, Kucera O, Labieniec-Watala M, Lai N, Laner V, Larsen TS, Lee HK, Lemieux H, Lerfall J, Lucchinetti E, MacMillan-Crow LA, Makrecka-Kuka M, Meszaros AT, Michalak S, Moiso N, Molina AJA, Montaigne D, Moore AL, Moreira BP, Mracek T, Muntane J, Muntean DM, Murray AJ, Nedergaard J, Nemec M, Newsom S, Nozickova K, O'Gorman D, Oliveira PF, Oliveira PJ, Orynbayeva Z, Pak YK, Palmeira CM, Patel HH, Pecina P, Pereira da Silva Grilo da Silva F, Pesta D, Petit PX, Pichaud N, Pirkmajer S, Porter RK, Pranger F, Prochownik EV, Puurand M, Radenkovic F, Reboredo P, Renner-Sattler K, Robinson MM, Rohlena J, Røslund GV, Rossiter HB, Rybacka-Mossakowska J, Saada A, Salvadego D, Scatena R, Schartner M, Scheibye-Knudsen M, Schilling JM, Schlattner U, Schoenfeld P, Scott GR, Shabalina IG, Sharma P, Shevchuk I, Siewiera K, Singer D, Sobotka O, Sokolova I, Spinazzi M, Stankova P, Stier A, Stocker R, Sumbalova Z, Suravajhala P, Tanaka M, Tandler B, Tepp K, Tomar D, Towheed A, Tretter L, Trivigno C, Tronstad KJ, Trougakos IP, Tyrrell DJ, Urban T, Valentine JM, Velika B, Vendelin M, Vercesi AE, Victor VM, Villena JA, Wagner BA, Ward ML, Watala C, Wei YH, Wieckowski MR, Wohlwend M, Wolff J, Wuest RCI, Zaugg K, Zaugg M, Zorzano A

Supporting co-authors:

Bakker BM, Bernardi P, Boetker HE, Borsheim E, Bouitbir J, Calbet JA, Calzia E, Chaurasia B, Clementi E, Coker RH, Collin A, Das AM, De Palma C, Dubouchaud H, Durham WJ, Dyrstad SE, Engin AB, Fornaro M, Gan Z, Garlid KD, Garten A, Gourlay CW, Granata C, Haas CB, Haavik J, Haendeler J, Hand SC, Hepple RT, Hickey AJ, Hoel F, Jang DH, Kainulainen H, Khamoui AV, Klingenspor M, Koopman WJH, Kowaltowski AJ, Krajcova A, Lane N, Lenaz G, Malik A, Markova M, Mazat JP, Menze MA, Methner A, Neuzil J, Oliveira MT, Pallotta ML, Parajuli N, Pettersen IKN, Porter C, Pulinilkunnil T, Ropelle ER, Salin K, Sandi C, Sazanov LA, Silber AM, Skolik R, Smenes BT, Soares FAA, Sonkar VK, Swerdlow RH, Szabo I, Trifunovic A, Thyfault JP, Vieyra A, Votion DM, Williams C, Zischka H

Updates and discussion:

http://www.mitoeagle.org/index.php/MitoEAGLE_preprint_2018-02-08

Correspondence: Gnaiger E

Chair COST Action CA15203 MitoEAGLE – <http://www.mitoeagle.org>

Department of Visceral, Transplant and Thoracic Surgery, D. Swarovski Research
Laboratory, Medical University of Innsbruck, Innrain 66/4, A-6020 Innsbruck, Austria

Email: erich.gnaiger@i-med.ac.at

Tel: +43 512 566796, Fax: +43 512 566796 20

Contents**Abstract****Executive summary****1. Introduction** – Box 1: In brief: Mitochondria and Bioblasts**2. Oxidative phosphorylation and coupling states in mitochondrial preparations**

Mitochondrial preparations

2.1. Three coupling states of mitochondrial preparations and residual oxygen consumption

Respiratory capacities in coupling control states

Kinetic control

The steady-state

Specification of biochemical dose

Phosphorylation, P»

Coupling – Uncoupling

LEAK, OXPHOS, ET, ROX

2.2. Coupling states and respiratory rates

P»/O₂ ratio

Control and regulation

Respiratory control and response

Respiratory coupling control

ET-pathway control states

2.3. Classical terminology for isolated mitochondria

States 1–5

3. Normalization: fluxes and flows*3.1. Normalization: system or sample*

Flow per system, I

Extensive quantities

Size-specific quantities – Box 2: Metabolic fluxes and flows: vectorial and scalar

3.2. Normalization for system-size: flux per chamber volume

System-specific flux, J

3.3. Normalization: per sample

Sample concentration, C_{mX}

Mass-specific flux, J_{mX,O_2}

Number concentration, C_{NX}

Flow per object, I_{X,O_2}

3.4. Normalization for mitochondrial content

Mitochondrial concentration, C_{mtE} , and mitochondrial markers

Mitochondria-specific flux, J_{mtE,O_2}

*3.5. Evaluation of mitochondrial markers**3.6. Conversion: units***4. Conclusions** – Box 3: Mitochondrial and cell respiration**5. References**

104 **Abstract** As the knowledge base and importance of mitochondrial physiology to human health
105 expand, the necessity for harmonizing nomenclature concerning mitochondrial respiratory
106 states and rates has become increasingly apparent. Clarity of concept and consistency of
107 nomenclature are key trademarks of a research field. These trademarks facilitate effective
108 transdisciplinary communication, education, and ultimately further discovery. Peter Mitchell's
109 chemiosmotic theory establishes the mechanism of energy transformation and coupling in
110 oxidative phosphorylation. The unifying concept of the protonmotive force provides the
111 framework for developing a consistent theory and nomenclature for mitochondrial physiology
112 and bioenergetics. Herein, we follow IUPAC guidelines on general terms of physical chemistry,
113 extended by considerations on open systems and irreversible thermodynamics. We align the
114 nomenclature and symbols of classical bioenergetics with a concept-driven constructive
115 terminology to express the meaning of each quantity clearly and consistently. In this position
116 statement, in the frame of COST Action MitoEAGLE, we endeavour to provide a balanced
117 view on mitochondrial respiratory control and a critical discussion on reporting data of
118 mitochondrial respiration in terms of metabolic flows and fluxes. Uniform standards for
119 evaluation of respiratory states and rates will ultimately support the development of databases
120 of mitochondrial respiratory function in species, tissues, and cells.

121

122 *Keywords:* Mitochondrial respiratory control, coupling control, mitochondrial
123 preparations, protonmotive force, oxidative phosphorylation, OXPHOS, efficiency, electron
124 transfer, ET; proton leak, LEAK, residual oxygen consumption, ROX, State 2, State 3, State 4,
125 normalization, flow, flux

126

127

128

129 **Executive summary**

130

131

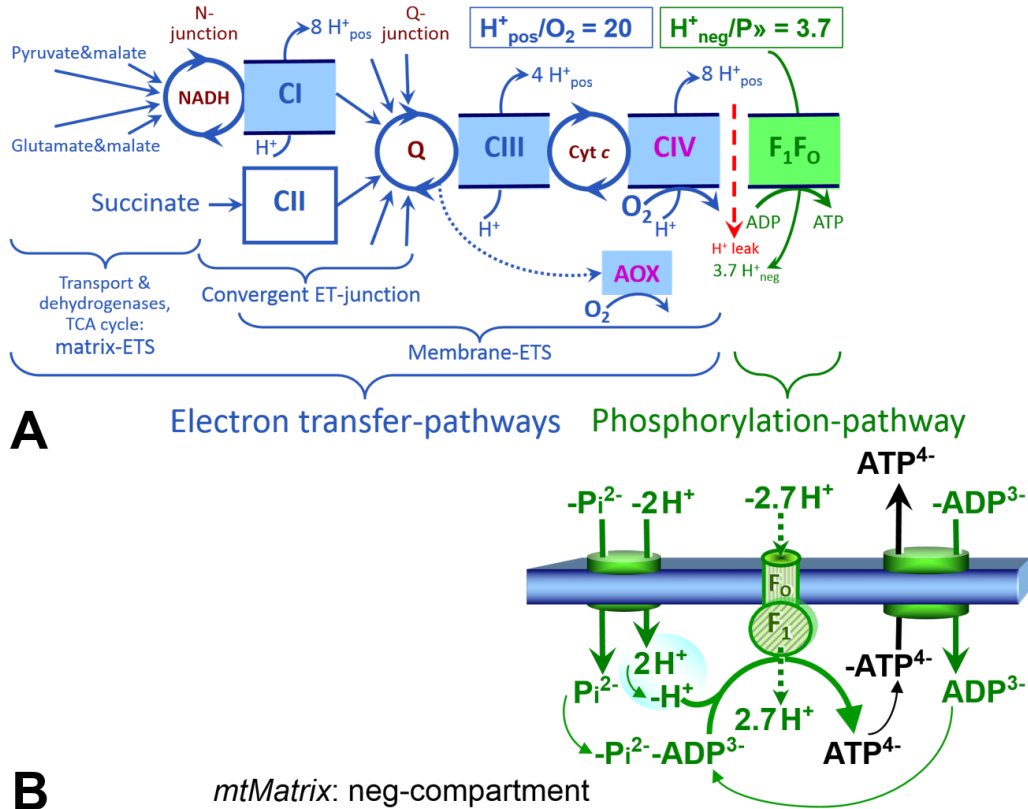
132 1. In view of broad implications on health care, mitochondrial researchers face an
133 increasing responsibility to disseminate their fundamental knowledge and novel
134 discoveries to a wide range of stakeholders and scientists beyond the group of
135 specialists. This requires implementation of a commonly accepted terminology
136 within the discipline and standardization in the translational context. Authors,
137 reviewers, journal editors, and lecturers are challenged to collaborate with the aim
138 to harmonize the nomenclature in the growing field of mitochondrial physiology
and bioenergetics.

139 2. Aerobic energy metabolism in mammalian mitochondria depends on the coupling of
140 ADP → ATP phosphorylation to oxygen consumption in catabolic reactions. In this
141 process of oxidative phosphorylation, coupling is mediated by translocation of
142 protons through respiratory proton pumps operating across the inner mitochondrial
143 membrane and generating or utilizing the protonmotive force measured between
144 the mitochondrial matrix and intermembrane compartment. Compartmental—or
145 vectorial—coupling thus distinguishes respiration from fermentation as the
146 counterpart of cellular core energy metabolism.

147 3. To exclude fermentation and other cytosolic interactions from exerting an effect on
148 mitochondrial metabolism, the barrier function of the plasma membrane must be
149 disrupted. Selective removal or permeabilization of the plasma membrane yields
150 mitochondrial preparations—including isolated mitochondria, tissue and cellular
151 preparations—with structural and functional integrity. Then extra-mitochondrial
152 concentrations of fuel substrates transported into the mitochondrial matrix, ADP,
153 ATP, inorganic phosphate, and cations including H⁺ can be controlled to
154 determine mitochondrial function under a set of conditions defined as coupling

155
156
157
158
159

control states. A concept-driven terminology of bioenergetics incorporates in its terms and symbols explicitly information on the nature of respiratory states, that makes the technical terms readily recognized and easy to understand.



160
161
162
163
164
165
166
167
168
169
170
171
172
173
174
175
176
177
178
179
180
181
182

Fig. 1. The oxidative phosphorylation (OXPHOS) system. (A) The mitochondrial electron transfer system (ETS) is fuelled by diffusion and transport of substrates across the mtOM and mtIM and consists of the matrix-ETS and membrane-ETS. ET-pathways are coupled to the phosphorylation-pathway. ET-pathways converge at the N-junction and Q-junction (additional arrows indicate electron entry into the Q-junction through electron transferring flavoprotein, glycerophosphate dehydrogenase, dihydro-orotate dehydrogenase, choline dehydrogenase, and sulfide-ubiquinone oxidoreductase). The dotted arrow indicates the branched pathway of oxygen consumption by alternative quinol oxidase (AOX). The H^+_{pos}/O_2 ratio is the outward proton flux from the matrix space to the positively (pos) charged compartment, divided by catabolic O_2 flux in the NADH-pathway. The H^+_{neg}/P ratio is the inward proton flux from the inter-membrane space to the negatively (neg) charged matrix space, divided by the flux of phosphorylation of ADP to ATP (Eq. 1). Due to ion leaks and proton slip these are not fixed stoichiometries. (B) Phosphorylation-pathway catalyzed by the proton pump F₁F₀-ATPase, adenine nucleotide translocase, and inorganic phosphate transporter. The H^+_{neg}/P stoichiometry is the sum of the coupling stoichiometry in the F₁F₀-ATPase reaction ($-2.7 H^+_{pos}$ from the positive intermembrane space, $2.7 H^+_{neg}$ to the matrix, *i.e.*, the negative compartment) and the proton balance in the translocation of ADP²⁻, ATP³⁻ and Pi²⁻. Modified from (A) Lemieux *et al.* (2017) and (B) Gnaiger (2014).

4. Mitochondrial coupling states are defined according to the control of respiratory oxygen consumption by the protonmotive force. Capacities of oxidative phosphorylation and electron transfer capacities are measured at kinetically saturating

- 183 concentrations of fuel substrates, ADP and inorganic phosphate, or at optimal
184 uncoupler concentrations, respectively. Respiratory capacities are a measure of the
185 upper bound of the rates of respiration, providing reference values for the diagnosis
186 of health and disease, and for evaluation of the effects of Evolutionary background,
187 Age, Gender and sex, Lifestyle and Environment (EAGLE).
- 188 5. Some degree of uncoupling is a characteristic of energy-transformations across
189 membranes. Uncoupling is caused by a variety of physiological, pathological,
190 toxicological, pharmacological and environmental conditions that exert an
191 influence not only on the proton leak and cation cycling, but also on proton slip
192 within the proton pumps and the structural integrity of the mitochondria. A more
193 loosely coupled state is induced by stimulation of mitochondrial superoxide anion
194 radical formation and the bypass of proton pumps. In addition, uncoupling by
195 application of protonophores represents an experimental intervention for the
196 transition from a well-coupled to the noncoupled state of mitochondrial respiration.
- 197 6. Respiratory oxygen consumption rates have to be carefully normalized to provide valid
198 information and enable meta-analytic studies beyond the specific question of a
199 particular experiment. Therefore, all raw data should be published in a supplemental
200 table or open access data repository. Normalization of rates for the volume of the
201 experimental chamber (the measuring system) is distinguished from normalization
202 for (1) the volume or mass of the experimental sample, (2) the number of objects
203 (cells, organisms), and (3) the concentration of mitochondrial markers in the
204 chamber.
- 205 7. The consistent use of terms and symbols discussed in this MitoEAGLE position
206 statement will facilitate transdisciplinary communication and support further
207 developments of a database on bioenergetics and mitochondrial physiology. The
208 present recommendations are focused on studies with mitochondrial preparations.
209 These will be extended in a series of reports on pathway control of mitochondrial
210 respiration, respiratory states in intact cells, and harmonization of experimental
211 procedures.
-

213 214 215 216 **Box 1: In brief – Mitochondria and Bioblasts**

217
218 **Mitochondria** are the oxygen-consuming electrochemical generators evolved from
219 endosymbiotic bacteria (Margulis 1970; Lane 2005). They were described by Richard Altmann
220 (1894) as ‘bioblasts’, which include not only the mitochondria as presently defined, but also
221 symbiotic and free-living bacteria. The word ‘mitochondria’ (Greek mitos: thread; chondros:
222 granule) was introduced by Carl Benda (1898).

223 Mitochondrial dysfunction is associated with a wide variety of genetic and degenerative
224 diseases. Robust mitochondrial function is supported by physical exercise and caloric balance,
225 and is central for sustained metabolic health throughout life. Therefore, a more consistent
226 presentation of mitochondrial physiology will improve our understanding of the etiology of
227 disease, the diagnostic repertoire of mitochondrial medicine, with a focus on protective
228 medicine, lifestyle and healthy aging.

229 We now recognize mitochondria as dynamic organelles with a double membrane that are
230 contained within eukaryotic cells. The mitochondrial inner membrane (mtIM) shows dynamic
231 tubular to disk-shaped cristae that separate the mitochondrial matrix, *i.e.*, the negatively charged
232 internal mitochondrial compartment, and the intermembrane space; the latter being positively
233 charged and enclosed by the mitochondrial outer membrane (mtOM). The mtIM contains the

234 non-bilayer phospholipid cardiolipin, which is not present in any other eukaryotic cellular
235 membrane. Cardiolipin promotes the formation of respiratory supercomplexes, which are
236 supramolecular assemblies based upon specific, though dynamic, interactions between
237 individual respiratory complexes (Greggio *et al.* 2017; Lenaz *et al.* 2017). Membrane fluidity
238 exerts an influence on functional properties of proteins incorporated in the membranes
239 (Waczulikova *et al.* 2007).

240 Mitochondria are the structural and functional elements of cell respiration. Cell
241 respiration is the consumption of oxygen by electron transfer coupled to electrochemical proton
242 translocation across the mtIM. In the process of oxidative phosphorylation (OXPHOS), the
243 reduction of O₂ is electrochemically coupled to the transformation of energy in the form of
244 adenosine triphosphate (ATP; Mitchell 1961, 2011). Mitochondria are the powerhouses of the
245 cell which contain the machinery of the OXPHOS-pathways, including transmembrane
246 respiratory complexes—proton pumps with FMN, Fe-S and cytochrome *b*, *c*, *aa₃* redox
247 systems); alternative dehydrogenases and oxidases; the coenzyme ubiquinone (Q); F₁F₀-
248 ATPase or ATP synthase; the enzymes of the tricarboxylic acid cycle and fatty acid oxidation;
249 transporters of ions, metabolites and co-factors; and mitochondrial kinases related to energy
250 transfer pathways. The mitochondrial proteome comprises over 1,200 proteins (Calvo *et al.*
251 2015; 2017), mostly encoded by nuclear DNA (nDNA), with a variety of functions, many of
252 which are relatively well known (*e.g.*, apoptosis-regulating proteins), while others are still under
253 investigation, or need to be identified (*e.g.*, alanine transporter).

254 There is a constant crosstalk between mitochondria and the other cellular components.
255 The crosstalk between mitochondria and endoplasmic reticulum is involved in the regulation of
256 calcium homeostasis, cell division, autophagy, differentiation, anti-viral signaling (Murley and
257 Nunnari 2016). Cellular mitostasis is maintained through regulation at both the transcriptional
258 and post-translational level, through cell signalling including proteostatic (*e.g.*, the ubiquitin-
259 proteasome and autophagy-lysosome pathways), and genome stability modules throughout the
260 cell cycle or even cell death, contributing to homeostatic regulation in response to varying
261 energy demands and stress (Quiros *et al.* 2016). In addition to mitochondrial movement along
262 the microtubules, mitochondrial morphology can change in response to energy requirements of
263 the cell via processes known as fusion and fission, through which mitochondria communicate
264 within a network, and in response to intracellular stress factors causing swelling and ultimately
265 permeability transition.

266 Mitochondria typically maintain several copies of their own genome known as
267 mitochondrial DNA (mtDNA; hundred to thousands per cell; Cummins 1998), which is
268 maternally inherited. One exception to strictly maternal inheritance in animals is found in
269 bivalves (Breton *et al.* 2007; White *et al.* 2008). mtDNA is 16.5 kB in length, contains 13
270 protein-coding genes for subunits of the transmembrane respiratory Complexes CI, CIII, CIV
271 and F₁F₀-ATPase, and also encodes 22 tRNAs and the mitochondrial 16S and 12S rRNA.
272 Additional gene content is encoded in the mitochondrial genome, *e.g.*, microRNAs, piRNA,
273 smithRNAs, repeat associated RNA, and even additional proteins (Duarte *et al.* 2014; Lee *et al.*
274 2015; Cobb *et al.* 2016). The mitochondrial genome is regulated and supplemented by
275 nuclear-encoded mitochondrial targeted proteins.

276 Abbreviation: mt, as generally used in mtDNA. Mitochondrion is singular and
277 mitochondria is plural.

278 ‘*For the physiologist, mitochondria afforded the first opportunity for an experimental*
279 *approach to structure-function relationships, in particular those involved in active transport,*
280 *vectorial metabolism, and metabolic control mechanisms on a subcellular level*’ (Ernster and
281 Schatz 1981).

282

283

284

285 1. Introduction

286

287 Mitochondria are the powerhouses of the cell with numerous physiological, molecular,
288 and genetic functions (**Box 1**). Every study of mitochondrial function and disease is faced with
289 **E**volution, **A**ge, **G**ender and sex, **L**ifestyle, and **E**nvironment (EAGLE) as essential background
290 conditions intrinsic to the individual patient or subject, cohort, species, tissue and to some extent
291 even cell line. As a large and highly coordinated group of laboratories and researchers, the
292 mission of the global MitoEAGLE Network is to generate the necessary scale, type, and quality
293 of consistent data sets and conditions to address this intrinsic complexity. Harmonization of
294 experimental protocols and implementation of a quality control and data management system
295 are required to interrelate results gathered across a spectrum of studies and to generate a
296 rigorously monitored database focused on mitochondrial respiratory function. In this way,
297 researchers within the same and across different disciplines will be positioned to compare
298 findings across traditions and generations to an agreed upon set of clearly defined and accepted
299 international standards.

300 Reliability and comparability of quantitative results depend on the accuracy of
301 measurements under strictly-defined conditions. A conceptual framework is required to warrant
302 meaningful interpretation and comparability of experimental outcomes carried out by research
303 groups at different institutes. With an emphasis on quality of research, collected data can be
304 useful far beyond the specific question of a particular experiment. Enabling meta-analytic
305 studies is the most economic way of providing robust answers to biological questions (Cooper
306 *et al.* 2009). Vague or ambiguous jargon can lead to confusion and may relegate valuable
307 signals to wasteful noise. For this reason, measured values must be expressed in standardized
308 units for each parameter used to define mitochondrial respiratory function. Standardization of
309 nomenclature and definition of technical terms are essential to improve the awareness of the
310 intricate meaning of current and past scientific vocabulary, for documentation and integration
311 into databases in general, and quantitative modelling in particular (Beard 2005). The focus on
312 coupling states and fluxes through metabolic pathways of aerobic energy transformation in
313 mitochondrial preparations is a first step in the attempt to generate a harmonized and
314 conceptually-oriented nomenclature in bioenergetics and mitochondrial physiology. Coupling
315 states of intact cells, the protonmotive force, and respiratory control by fuel substrates and
316 specific inhibitors of respiratory enzymes will be reviewed in subsequent communications.

317

318

319 2. Oxidative phosphorylation and coupling states in mitochondrial preparations

320 *‘Every professional group develops its own technical jargon for talking about matters of*
321 *critical concern ... People who know a word can share that idea with other members of*
322 *their group, and a shared vocabulary is part of the glue that holds people together and*
323 *allows them to create a shared culture’ (Miller 1991).*

324

325 **Mitochondrial preparations** are defined as either isolated mitochondria, or tissue and
326 cellular preparations in which the barrier function of the plasma membrane is disrupted. The
327 plasma membrane separates the cytosol, nucleus, and organelles (the intracellular
328 compartment) from the environment of the cell. The plasma membrane consists of a lipid
329 bilayer, embedded proteins, and attached organic molecules that collectively control the
330 selective permeability of ions, organic molecules, and particles across the cell boundary. The
331 intact plasma membrane, therefore, prevents the passage of many water-soluble mitochondrial
332 substrates—such as succinate or adenosine diphosphate (ADP), that are required for the
333 analysis of respiratory capacity at kinetically-saturating concentrations; this limits the scope of
334 investigations into mitochondrial respiratory function in intact cells. The cholesterol content of
335 the plasma membrane is high compared to mitochondrial membranes. Therefore, mild

336 detergents—such as digitonin and saponin—can be applied to selectively permeabilize the
 337 plasma membrane by interaction with cholesterol and allow free exchange of cytosolic
 338 components with ions and organic molecules of the immediate cell environment, while
 339 maintaining the integrity and localization of organelles, cytoskeleton, and the nucleus.
 340 Application of optimum concentrations of permeabilization agents (mild detergents or toxins)
 341 leads to the complete loss of cell viability, tested by nuclear staining and washout of cytosolic
 342 marker enzymes—such as lactate dehydrogenase, while mitochondrial function remains intact.
 343 The respiration rate of isolated mitochondria remains unaltered after the addition of low
 344 concentrations of digitonin or saponin. In addition to mechanical permeabilization during
 345 homogenization of tissue, permeabilization agents may be applied to ensure permeabilization
 346 of all cells. Suspensions of cells permeabilized in the respiration chamber and crude tissue
 347 homogenates contain all components of the cell at highly diluted concentrations. All
 348 mitochondria are retained in chemically-permeabilized mitochondrial preparations and crude
 349 tissue homogenates. In the preparation of isolated mitochondria, the cells or tissues are
 350 homogenized, and the mitochondria are separated from other cell fractions and purified by
 351 differential centrifugation, entailing the loss of a fraction of mitochondria. Typical
 352 mitochondrial recovery ranges from 30% to 80%. Maximization of the purity of isolated
 353 mitochondria may compromise not only the mitochondrial yield but also the structural and
 354 functional integrity. Therefore, protocols to isolate mitochondria need to be optimized
 355 according to each study. The term mitochondrial preparation does not include further
 356 fractionation of mitochondrial components, neither submitochondrial particles.

357

358 *2.1. Three coupling states of mitochondrial preparations and residual oxygen consumption*

359

360 **Respiratory capacities in coupling control states:** To extend the classical nomenclature
 361 on mitochondrial coupling states (Section 2.3) by a concept-driven terminology that
 362 incorporates explicitly information on the nature of respiratory states, the terminology must be
 363 general and not restricted to any particular experimental protocol or mitochondrial preparation
 364 (Gnaiger 2009). We focus primarily on the conceptual ‘why’, along with clarification of the
 365 experimental ‘how’. In the following section, the concept-driven terminology is explained and
 366 coupling states are defined. We define respiratory capacities, comparable to channel capacity
 367 in information theory (Schneider 2006), as the upper bound of the rate of respiration measured
 368 in defined coupling control states and electron transfer-pathway (ET-pathway) states.

369 To provide a diagnostic reference for respiratory capacities of core energy metabolism,
 370 the capacity of *oxidative phosphorylation*, OXPHOS, is measured at kinetically-saturating
 371 concentrations of ADP and inorganic phosphate, P_i . The *oxidative* ET-capacity reveals the
 372 limitation of OXPHOS-capacity mediated by the *phosphorylation*-pathway. The ET- and
 373 phosphorylation-pathways comprise coupled segments of the OXPHOS-system. ET-capacity
 374 is measured as noncoupled respiration by application of *external uncouplers*. The contribution
 375 of *intrinsically uncoupled* oxygen consumption is easily studied in the absence of ADP—by
 376 not stimulating phosphorylation, or by inhibition of the phosphorylation-pathway. The
 377 corresponding states are collectively classified as LEAK-states, when oxygen consumption
 378 compensates mainly for ion leaks, including the proton leak (**Table 1**). Defined coupling states
 379 are induced by: (1) adding cation chelators such as EGTA, binding free Ca^{2+} and thus limiting
 380 cation cycling; (2) adding ADP and P_i ; (3) inhibiting the phosphorylation-pathway; and (4)
 381 uncoupler titrations, while maintaining a defined ET-pathway state with constant fuel substrates
 382 and inhibitors of specific branches of the ET-pathway (**Fig. 1**).

383 **Kinetic control:** Coupling control states are established in the study of mitochondrial
 384 preparations to obtain reference values for various output variables. Physiological conditions *in*
 385 *vivo* deviate from these experimentally obtained states. Since kinetically-saturating
 386 concentrations, *e.g.*, of ADP or oxygen, may not apply to physiological intracellular conditions,

387 relevant information is obtained in studies of kinetic responses to intermediate conditions
 388 between the LEAK state at zero [ADP] and the OXPHOS-state at saturating [ADP], or of
 389 respiratory capacities in the range between kinetically-saturating [O₂] and anoxia (Gnaiger
 390 2001).

391 **The steady-state:** Mitochondria represent a thermodynamically open system in non-
 392 equilibrium states of biochemical energy transformation. State variables (protonmotive force;
 393 redox states) and metabolic *rates* (fluxes) are measured in defined mitochondrial respiratory
 394 *states*. Steady states can be obtained only in open systems, in which changes by *internal*
 395 transformations, *e.g.*, O₂ consumption, are instantaneously compensated for by *external* fluxes,
 396 *e.g.*, O₂ supply, preventing a change of oxygen concentration in the system (Gnaiger 1993b).
 397 Mitochondrial respiratory states monitored in closed systems satisfy the criteria of pseudo-
 398 steady states for limited periods of time, when changes in the system (concentrations of O₂,
 399 fuel substrates, ADP, P_i, H⁺) do not exert significant effects on metabolic fluxes (respiration,
 400 phosphorylation). Such pseudo-steady states require respiratory media with sufficient buffering
 401 capacity and kinetically-saturating concentrations of substrates to be maintained, and thus
 402 depend on the kinetics of the processes under investigation.

403

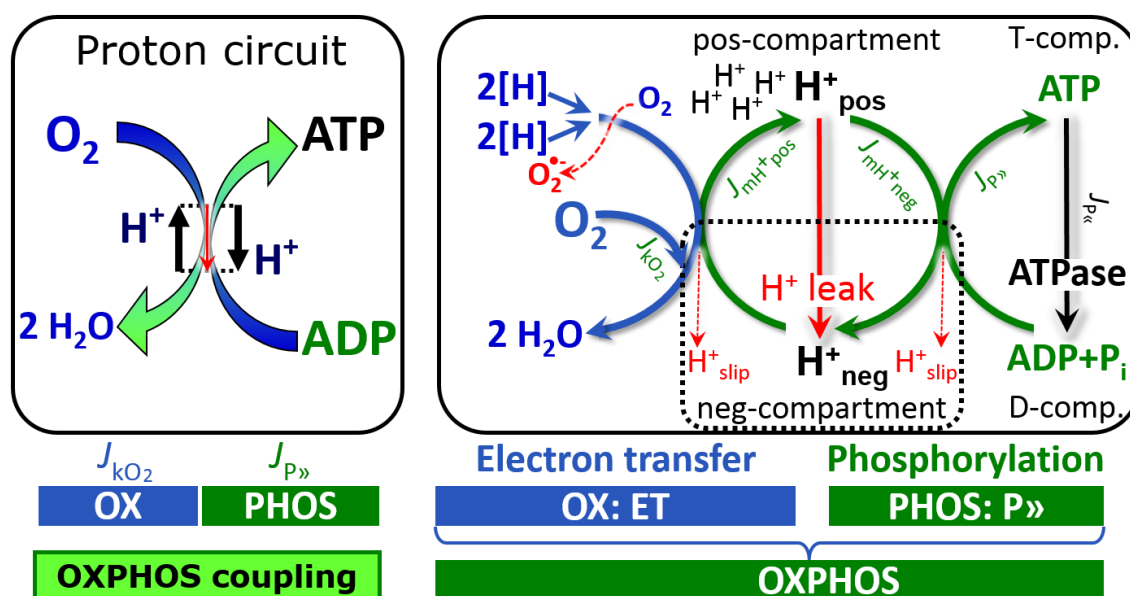
404 **Table 1. Coupling states and residual oxygen consumption in mitochondrial**
 405 **preparations in relation to respiration- and phosphorylation-rate, J_{kO_2} and $J_{P_{\gg}}$,**
 406 **and protonmotive force, pmf. Coupling states are established at kinetically-**
 407 **saturating concentrations of fuel substrates and O₂.**

State	J_{kO_2}	$J_{P_{\gg}}$	pmf	Inducing factors	Limiting factors
LEAK	L ; low, cation leak-dependent respiration	0	max.	proton leak, slip, and cation cycling	$J_{P_{\gg}} = 0$: (1) without ADP, L_N ; (2) max. ATP/ADP ratio, L_T ; or (3) inhibition of the phosphorylation-pathway, L_{Omy}
OXPHOS	P ; high, ADP-stimulated respiration	max.	high	kinetically-saturating [ADP] and [P _i]	$J_{P_{\gg}}$ by phosphorylation-pathway; or J_{kO_2} by ET-capacity
ET	E ; max., noncoupled respiration	0	low	optimal external uncoupler concentration for max. $J_{O_2,E}$	J_{kO_2} by ET-capacity
ROX	R_{ox} ; min., residual O ₂ consumption	0	0	$J_{O_2,R_{ox}}$ in non-ET-pathway oxidation reactions	full inhibition of ET-pathway; or absence of fuel substrates

408

409 **Specification of biochemical dose:** Substrates, uncouplers, inhibitors, and other
 410 biochemical reagents are titrated to dissect mitochondrial function. Nominal concentrations of
 411 these substances are usually reported as initial amount of substance concentration [mol·L⁻¹] in
 412 the incubation medium. When aiming at the measurement of kinetically saturated processes—
 413 such as OXPHOS-capacities, the concentrations for substrates can be chosen according to the
 414 apparent equilibrium constant, K_m' . In the case of hyperbolic kinetics, only 80% of maximum
 415 respiratory capacity is obtained at a substrate concentration of four times the K_m' , whereas
 416 substrate concentrations of 5, 9, 19 and 49 times the K_m' are theoretically required for reaching
 417 83%, 90%, 95% or 98% of the maximal rate (Gnaiger 2001). Other reagents are chosen to

418 inhibit or alter some process. The amount of these chemicals in an experimental incubation is
 419 selected to maximize effect, yet not lead to unacceptable off-target consequences that would
 420 adversely affect the data being sought. Specifying the amount of substance in an incubation as
 421 nominal concentration in the aqueous incubation medium can be ambiguous (Doskey *et al.*
 422 2015), particularly when lipophilic substances (oligomycin; uncouplers, permeabilization
 423 agents) or cations (TPP⁺; fluorescent dyes such as safranin, TMRM) are applied which
 424 accumulate in biological membranes or the mitochondrial matrix. For example, a dose of
 425 digitonin of 8 fmol·cell⁻¹ (10 μg·10⁻⁶ cells) is optimal for permeabilization of endothelial cells,
 426 and the concentration in the incubation medium has to be adjusted according to the cell density
 427 applied (Doerrier *et al.* 2018). Generally, dose/exposure can be specified per unit of biological
 428 sample, *i.e.*, (nominal moles of xenobiotic)/(number of cells) [mol·cell⁻¹] or, as appropriate, per
 429 mass of biological sample [mol·kg⁻¹]. This approach to specification of dose/exposure provides
 430 a scalable parameter that can be used to design experiments, help interpret a wide variety of
 431 experimental results, and provide absolute information that allows researchers worldwide to
 432 make the most use of published data (Doskey *et al.* 2015).
 433



434
 435 **Fig. 2. The proton circuit and coupling in oxidative phosphorylation (OXPHOS).** Oxygen
 436 flux, J_{kO_2} , through the catabolic ET-pathway, k , is coupled to flux through the phosphorylation-
 437 pathway of ADP to ATP, $J_{P\gg}$. The proton pumps of the ET-pathway drive proton flux into the
 438 positive (pos) compartment, J_{mH+pos} , which generates the output protonmotive force (motive,
 439 subscript m). F_1F_0 -ATPase is coupled to inward proton current into the negative (neg)
 440 compartment, J_{mH+neg} , to phosphorylate ADP+ P_i to ATP. 2[H] indicates the reduced hydrogen
 441 equivalents of fuel substrates of the catabolic reaction k with oxygen. Fluxes are expressed per
 442 volume, V [m³], of the system. The system defined by the boundaries (full black line) is not a
 443 black box, but is analysed as a compartmental system. The negative compartment (neg-
 444 compartment, enclosed by the dotted line) is the matrix space, separated by the mtIM from the
 445 positive compartment (pos-compartment). ADP+ P_i and ATP are the substrate- and product-
 446 compartments (scalar ADP and ATP compartments, D-comp. and T-comp.), respectively. At
 447 steady-state proton turnover, $J_{\infty H^+}$, and ATP turnover, $J_{\infty P}$, maintain concentrations constant,
 448 when $J_{mH+\infty} = J_{mH+pos} = J_{mH+neg}$, and $J_{P\infty} = J_{P\gg} = J_{P\ll}$. Modified from Gnaiger (2014).
 449

450 **Phosphorylation, P \gg :** *Phosphorylation* in the context of OXPHOS is defined as
 451 phosphorylation of ADP by P_i to ATP. On the other hand, the term phosphorylation is used
 452 generally in many contexts, *e.g.*, protein phosphorylation. This justifies consideration of a

453 symbol more discriminating and specific than P as used in the P/O ratio (phosphate to atomic
 454 oxygen ratio; $O = 0.5 O_2$), where P indicates phosphorylation of ADP to ATP or GDP to GTP.
 455 We propose the symbol P» for the endergonic (uphill) direction of phosphorylation
 456 $ADP \rightarrow ATP$, and likewise the symbol P« for the corresponding exergonic (downhill) hydrolysis
 457 $ATP \rightarrow ADP$ (Fig. 2). P» refers mainly to electrontransfer phosphorylation but may also involve
 458 substrate-level phosphorylation as part of the tricarboxylic acid (TCA) cycle (succinyl-CoA
 459 ligase) and phosphorylation of ADP catalyzed by phosphoenolpyruvate carboxykinase.
 460 Transphosphorylation is performed by adenylate kinase, creatine kinase, hexokinase and
 461 nucleoside diphosphate kinase. In isolated mammalian mitochondria, ATP production
 462 catalyzed by adenylate kinase ($2 ADP \leftrightarrow ATP + AMP$) proceeds without fuel substrates in the
 463 presence of ADP (Komlódi and Tretter 2017). Kinase cycles are involved in intracellular energy
 464 transfer and signal transduction for regulation of energy flux.

465 **Coupling:** In mitochondrial electron transfer (Fig. 1), vectorial transmembrane proton
 466 flux is coupled through the proton pumps CI, CIII and CIV to the catabolic flux of scalar
 467 reactions, collectively measured as oxygen flux (Fig. 2). Thus mitochondria are elements of
 468 energy transformation. Energy cannot be lost or produced in any internal process (First Law of
 469 thermodynamics). Open and closed systems can gain or loose energy only by external fluxes—
 470 by exchange with the environment. Energy is a conserved quantity. Therefore, energy can
 471 neither be produced by mitochondria, nor is there any internal process without energy
 472 conservation. Exergy is defined as the ‘free energy’ with the potential to perform work.
 473 *Coupling* is the mechanistic linkage of an exergonic process (spontaneous, negative exergy
 474 change) with an endergonic process (positive exergy change) in energy transformations which
 475 conserve part of the exergy that would be irreversible lost or dissipated in an uncoupled process.

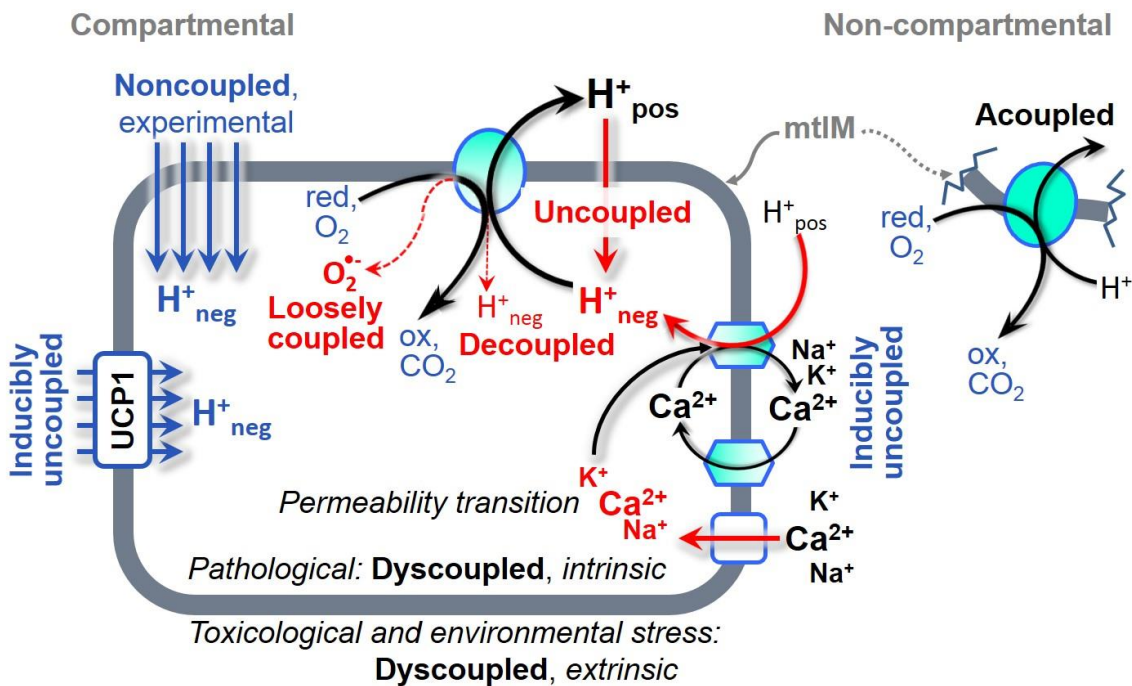
476 **Uncoupling:** Uncoupling of mitochondrial respiration is a general term comprising
 477 diverse mechanisms. Differences of terms—uncoupled vs. noncoupled—are easily overlooked,
 478 although they relate to different mechanisms of uncoupling (Fig. 3). Rigorous definitions are
 479 required to clarify the concepts (Table 2).

- 480 1. Proton leak across the mtIM from the pos– to the neg–compartment (Fig. 2);
- 481 2. Cycling of other cations, strongly stimulated by permeability transition;
- 482 3. Proton slip in the proton pumps when protons are effectively not pumped (CI, CIII and
 483 CIV) or are not driving phosphorylation (F_1F_0 -ATPase);
- 484 4. Loss of compartmental integrity when electron transfer is acoupled;
- 485 5. Electron leak in the loosely coupled univalent reduction of oxygen (O_2 ; dioxygen) to
 486 superoxide ($O_2^{\cdot -}$; superoxide anion radical).

487
 488 **LEAK-state (Fig. 4A):** The LEAK-state is defined as a state of mitochondrial respiration
 489 when O_2 flux mainly compensates for ion leaks in the absence of ATP synthesis, at kinetically-
 490 saturating concentrations of O_2 and respiratory fuel substrates. LEAK-respiration is measured
 491 to obtain an estimate of *intrinsic uncoupling* without addition of an experimental uncoupler: (1)
 492 in the absence of adenylates; (2) after depletion of ADP at a maximum ATP/ADP ratio; or (3)
 493 after inhibition of the phosphorylation-pathway by inhibitors of F_1F_0 -ATPase—such as
 494 oligomycin, or of adenine nucleotide translocase—such as carboxyatractyloside. Adjustment
 495 of the nominal concentration of these inhibitors to the density of biological sample applied can
 496 minimize or avoid inhibitory side-effects exerted on ET-capacity or even some dyscoupling.

497 **Proton leak and uncoupled respiration:** Proton leak is a leak current of protons. The
 498 intrinsic proton leak is the *uncoupled* process in which protons diffuse across the mtIM in the
 499 dissipative direction of the downhill protonmotive force without coupling to phosphorylation
 500 (Fig. 4A). The proton leak flux depends non-linearly on the protonmotive force (Garlid *et al.*
 501 1989; Divakaruni and Brand 2011), it is a property of the mtIM and may be enhanced due to
 502 possible contaminations by free fatty acids. Inducible uncoupling mediated by uncoupling
 503 protein 1 (UCP1) is physiologically controlled, *e.g.*, in brown adipose tissue. UCP1 is a member

504 of the mitochondrial carrier family which is involved in the translocation of protons across the
 505 mtIM (Klingenberg 2017). Consequently, the short-circuit diminishes the protonmotive force
 506 and stimulates electron transfer to O₂ and heat dissipation without phosphorylation of ADP.
 507



508
 509 **Fig 3. Mechanisms of respiratory uncoupling.** An intact mitochondrial inner membrane,
 510 mtIM, is required for vectorial, compartmental coupling. ‘Acoupled’ respiration is the
 511 consequence of structural disruption with catalytic activity of non-compartmental
 512 mitochondrial fragments. Inducibly uncoupled (activation of UCP1) and experimentally
 513 noncoupled respiration (titration of protonophores) stimulate respiration to maximum oxygen
 514 flux of ET-capacity. Uncoupled, decoupled, and loosely coupled respiration are components of
 515 intrinsic LEAK respiration. Pathological dysfunction may affect all types of uncoupling,
 516 including permeability transition, causing intrinsically dyscoupled respiration. Similarly,
 517 toxicological and environmental stress factors can cause extrinsically dyscoupled respiration.
 518

519 **Cation cycling:** There can be other cation contributors to leak current including calcium
 520 and probably magnesium. Calcium current is balanced by mitochondrial Na⁺/Ca²⁺ exchange,
 521 which is balanced by Na⁺/H⁺ or K⁺/H⁺ exchanges. This is another effective uncoupling
 522 mechanism different from proton leak.

523 **Proton slip and decoupled respiration:** Proton slip is the *decoupled* process in which
 524 protons are only partially translocated by a proton pump of the ET-pathways and slip back to
 525 the original compartment. The proton leak is the dominant contributor to the overall leak current
 526 in mammalian mitochondria incubated under physiological conditions at 37 °C, whereas proton
 527 slip is increased at lower experimental temperature (Canton *et al.* 1995). Proton slip can also
 528 happen in association with the F₁F₀-ATPase, in which the proton slips downhill across the
 529 pump to the matrix without contributing to ATP synthesis. In each case, proton slip is a property
 530 of the proton pump and increases with the pump turnover rate.

531 **Electron leak and loosely coupled respiration:** Superoxide production by the ETS leads
 532 to a bypass of proton pumps and correspondingly lower P_o/O₂ ratio. This depends on the actual
 533 site of electron leak and the scavenging of hydrogen peroxide by cytochrome *c*, whereby
 534 electrons may re-enter the ETS with proton translocation by CIV.


535 **Loss of compartmental integrity and acoupled respiration:** Electron transfer and O₂
 536 consumption proceed without compartmental proton translocation in disrupted mitochondrial

537 fragments. Such fragments form during mitochondrial isolation, and may not fully fuse to re-
 538 establish structurally intact mitochondria. Loss of mtIM integrity, therefore, is the cause of
 539 acoupled respiration, which is a nonvectorial dissipative process without control by the
 540 protonmotive force.

541 **Dyscoupled respiration:** Mitochondrial injuries may lead to *dyscoupling* as a
 542 pathological or toxicological cause of *uncoupled* respiration. Dyscoupling may involve any
 543 type of uncoupling mechanism, *e.g.*, opening the permeability transition pore. Dyscoupled
 544 respiration is distinguished from the experimentally induced *noncoupled* respiration in the ET-
 545 state (**Fig. 3**).

546

547 **Table 2. Distinction of terms related to respiratory coupling and uncoupling**
 548 **(Fig. 3).**

Term	J_{KO_2}	$P \gg O_2$	Note	
acoupled		0	electron transfer in mitochondrial fragments without vectorial proton translocation	
uncoupled	L	0	non-phosphorylating LEAK-respiration	
intrinsic, no protonophore added		ion leak	0	component of LEAK-respiration, uncoupled <i>sui generis</i> , ion diffusion across the mtIM
		decoupled	0	component of LEAK-respiration, proton slip
		loosely coupled	0	component of LEAK-respiration, lower coupling due to superoxide formation and bypass of proton pumps
		dyscoupled	0	pathologically, toxicologically, environmentally increased uncoupling, mitochondrial dysfunction
		inducibly uncoupled	E	0
noncoupled	E	0	non-phosphorylating respiration stimulated to maximum flux at optimum exogenous uncoupler concentration (Fig. 4C)	
well-coupled	P	high	phosphorylating respiration with an intrinsic LEAK component (Fig. 4B)	
fully coupled	$P - L$	max.	OXPHOS-capacity corrected for LEAK-respiration (Fig. 5)	

549

550 **OXPHOS-state (Fig. 4B):** The OXPHOS-state is defined as the respiratory state with
 551 kinetically-saturating concentrations of O_2 , respiratory and phosphorylation substrates, and
 552 absence of exogenous uncoupler, which provides an estimate of the maximal respiratory
 553 capacity in the OXPHOS-state for any given ET-pathway state. Respiratory capacities at
 554 kinetically-saturating substrate concentrations provide reference values or upper limits of
 555 performance, aiming at the generation of data sets for comparative purposes. Physiological
 556 activities and effects of substrate kinetics can be evaluated relative to the OXPHOS-capacity.

557 As discussed previously, 0.2 mM ADP does not fully saturate flux in isolated
 558 mitochondria (Gnaiger 2001; Puchowicz *et al.* 2004); greater ADP concentration is required,
 559 particularly in permeabilized muscle fibres and cardiomyocytes, to overcome limitations by
 560 intracellular diffusion and by the reduced conductance of the mtOM (Jepihhina *et al.* 2011,
 561 Illaste *et al.* 2012, Simson *et al.* 2016), either through interaction with tubulin (Rostovtseva *et al.*
 562 2008) or other intracellular structures (Birkedal *et al.* 2014). In permeabilized muscle fibre

563 bundles of high respiratory capacity, the apparent K_m for ADP increases up to 0.5 mM (Saks *et al.* 1998), consistent with experimental evidence that >90% saturation is reached only at >5
 564 mM ADP (Pesta and Gnaiger 2012). Similar ADP concentrations are also required for accurate
 565 determination of OXPHOS-capacity in human clinical cancer samples and permeabilized cells
 566 (Klepinin *et al.* 2016; Koit *et al.* 2017). Whereas 2.5 to 5 mM ADP is sufficient to obtain the
 567 actual OXPHOS-capacity in many types of permeabilized tissue and cell preparations,
 568 experimental validation is required in each specific case.
 569

571 **Electron transfer-state**
 572 (Fig. 4C): The ET-state is defined as the *noncoupled* state
 573 with kinetically-saturating
 574 concentrations of O_2 , respiratory
 575 substrate and optimum
 576 *exogenous* uncoupler
 577 concentration for maximum O_2
 578 flux, as an estimate of ET-
 579 capacity. Inhibition of respiration
 580 is observed at higher than
 581 optimum uncoupler
 582 concentrations. As a
 583 consequence of the nearly
 584 collapsed protonmotive force, the
 585 driving force is insufficient for
 586 phosphorylation, and $J_{P_{\gg}} = 0$.
 587

588
 589 Besides the three
 590 fundamental coupling states of
 591 mitochondrial preparations, the
 592 following respiratory state is
 593 relevant to assess respiratory
 594 function:

595 **ROX state and *Rox*:** The
 596 rate of residual oxygen
 597 consumption, *Rox*, is defined as
 598 O_2 consumption due to oxidative
 599 side reactions remaining after
 600 inhibition of ET—with rotenone,
 601 malonic acid and antimycin A.
 602 Cyanide and azide not only
 603 inhibit CIV but also several
 604 peroxidases involved in *Rox*.
 605 ROX is not a coupling state. *Rox*
 606 represents a baseline that is used
 607 to correct mitochondrial
 608 respiration in defined coupling
 609 states. *Rox* is not necessarily
 610 equivalent to non-mitochondrial
 611 respiration, considering oxygen-
 612 consuming reactions in
 613 mitochondria not related to ET—such as oxygen consumption in reactions catalyzed by

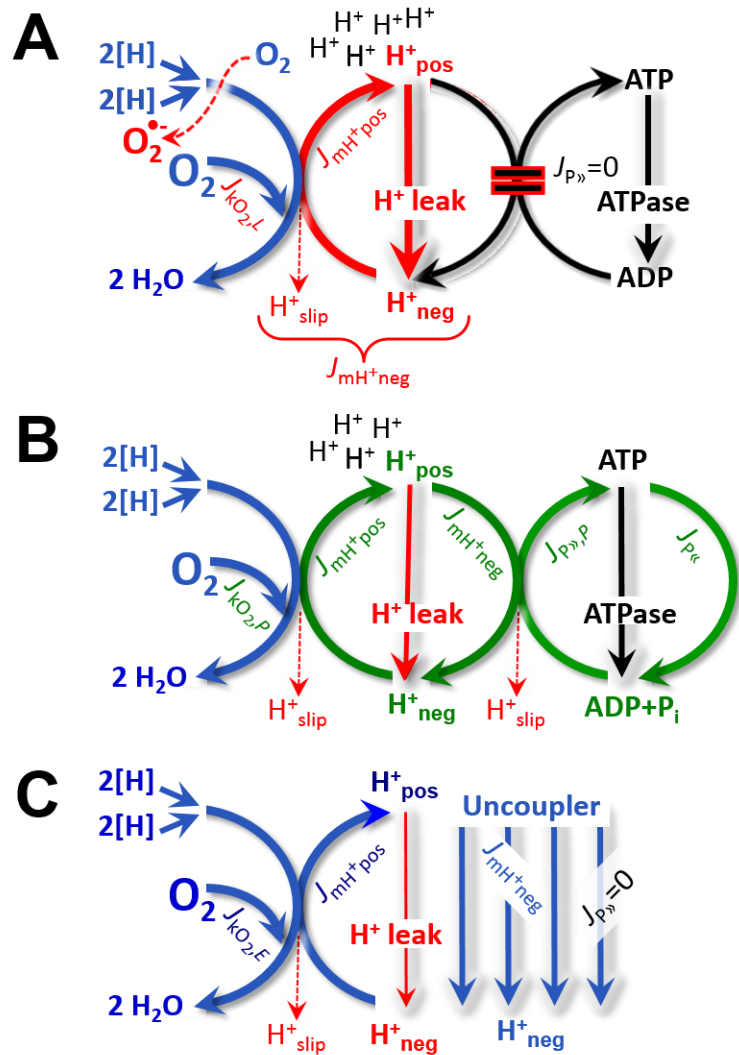


Fig. 4. Respiratory coupling states. A: LEAK-state:

Phosphorylation is arrested, $J_{P_{\gg}} = 0$, and catabolic oxygen flux, $J_{kO_2,L}$, is controlled mainly by the proton leak, $J_{mH^{+neg,L}}$, at maximum protonmotive force (Fig. 3). **B: OXPHOS-state:** Phosphorylation, $J_{P_{\gg}}$, is stimulated by kinetically-saturating [ADP] and inorganic phosphate, $[P_i]$, and is supported by a high protonmotive force. O_2 flux, $J_{kO_2,P}$, is well-coupled at a P_{\gg}/O_2 ratio of $J_{P_{\gg},P}/J_{O_2,P}$. **C: ET-state:** Noncoupled respiration, $J_{kO_2,E}$, is maximum at optimum exogenous uncoupler concentration and phosphorylation is zero, $J_{P_{\gg}} = 0$. See also Fig. 2.

614 monoamine oxidases (type A and B), monooxygenases (cytochrome P450 monooxygenases),
 615 dioxygenase (sulfur dioxygenase and trimethyllysine dioxygenase), and several hydroxylases.
 616 Mitochondrial preparations, especially those obtained from liver, may be contaminated by
 617 peroxisomes. This fact makes the exact determination of mitochondrial oxygen consumption
 618 and mitochondria-associated generation of reactive oxygen species complicated (Schönfeld *et*
 619 *al.* 2009). The dependence of ROX-linked oxygen consumption needs to be studied in detail
 620 together with non-ET enzyme activities, availability of specific substrates, oxygen
 621 concentration, and electron leakage leading to the formation of reactive oxygen species.

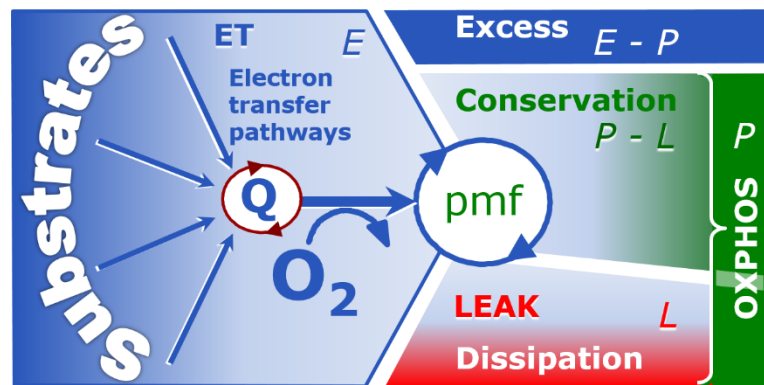
622 2.2. Coupling states and respiratory rates

623
 624
 625 As an improvement of previous terminologies, we distinguish metabolic *pathways* from
 626 metabolic *states* and the corresponding metabolic *rates*; for example: ET-pathways (**Fig. 5**),
 627 ET-state (**Fig. 4C**), and ET-capacity, E , respectively (**Table 1**). The protonmotive force is *high*
 628 in the OXPHOS-state when it drives phosphorylation, *maximum* in the LEAK-state of coupled
 629 mitochondria, driven by LEAK-respiration at a minimum back flux of cations to the matrix
 630 side, and *very low* in the ET-state when uncouplers short-circuit the proton cycle (**Table 1**).

631 The three coupling states, ET, LEAK and OXPHOS, are shown schematically with the
 632 corresponding respiratory rates, abbreviated as E , L and P , respectively (**Fig. 5**).

633
 634 **Fig. 5. Four-compartment**

635 **model of oxidative**
 636 **phosphorylation.** Respiratory
 637 states (ET, OXPHOS, LEAK)
 638 and corresponding rates (E , P , L)
 639 are connected by the
 640 protonmotive force, pmf.
 641 Electron transfer-capacity, E , is
 642 partitioned into (1) dissipative
 643 LEAK-respiration, L , when the
 644 Gibbs energy change of catabolic
 645 O_2 consumption is irreversibly lost, (2) net OXPHOS-capacity, $P-L$, with partial conservation
 646 of the capacity to perform work, and (3) the excess capacity, $E-P$. Modified from Gnaiger
 647 (2014).



648
 649 E may exceed or be equal to P . $E > P$ is observed in many types of mitochondria, varying
 650 between species, tissues and cell types (Gnaiger 2009). $E - P$ is the excess ET-capacity pushing
 651 the phosphorylation-flux (**Fig. 1B**) to the limit of its *capacity of utilizing* the protonmotive force.
 652 In addition, the magnitude of $E - P$ depends on the tightness of respiratory coupling or degree of
 653 uncoupling, since an increase of L causes P to increase towards the limit of E . The *excess* $E - P$
 654 capacity, $E - P$, therefore, provides a sensitive diagnostic indicator of specific injuries of the
 655 phosphorylation-pathway, under conditions when E remains constant but P declines relative to
 656 controls (**Fig. 5**). Substrate cocktails supporting simultaneous convergent electron transfer to
 657 the Q-junction for reconstitution of TCA cycle function establish pathway control states with
 658 high ET-capacity, and consequently increase the sensitivity of the $E - P$ assay.

659 E cannot theoretically be lower than P . $E < P$ must be discounted as an artefact, which
 660 may be caused experimentally by: (1) loss of oxidative capacity during the time course of the
 661 respirometric assay, since E is measured subsequently to P ; (2) using insufficient uncoupler
 662 concentrations; (3) using high uncoupler concentrations which inhibit ET (Gnaiger 2008); (4)
 663 high oligomycin concentrations applied for measurement of L before titrations of uncoupler,

664 when oligomycin exerts an inhibitory effect on *E*. On the other hand, the excess ET-capacity is
 665 overestimated if non-saturating [ADP] or [P_i] are used. See State 3 in the next section.

666 **P_»/O₂ ratio:** The P_»/O₂ ratio (P_»/4 e⁻) is two times the ‘P/O’ ratio (P_»/2 e⁻) of classical
 667 bioenergetics. P_»/O₂ is a generalized symbol, independent phosphorylation assessment by
 668 determination of P_i consumption (P_i/O₂ flux ratio), ADP depletion (ADP/O₂ flux ratio), or ATP
 669 production (ATP/O₂ flux ratio).

670 The mechanistic P_»/O₂ ratio—or P_»/O₂ stoichiometry—is calculated from the proton-to-
 671 oxygen and proton-to-phosphorylation coupling stoichiometries (**Fig. 1A**),
 672

$$673 \quad P_{\gg}/O_2 = \frac{H_{\text{pos}}^+/O_2}{H_{\text{neg}}^+/P_{\gg}} \quad (1)$$

674
 675 The H⁺_{pos}/O₂ *coupling stoichiometry* (referring to the full 4 electron reduction of O₂) depends
 676 on the ET-pathway control state which defines the relative involvement of the three coupling
 677 sites (CI, CIII and CIV) in the catabolic pathway of electrons to O₂. This varies with: (1) a
 678 bypass of CI by single or multiple electron input into the Q-junction; and (2) a bypass of CIV
 679 by involvement of AOX. H⁺_{pos}/O₂ is 12 in the ET-pathways involving CIII and CIV as proton
 680 pumps, increasing to 20 for the NADH-pathway (**Fig. 1A**), but a general consensus on H⁺_{pos}/O₂
 681 stoichiometries remains to be reached (Hinkle 2005; Wikström and Hummer 2012; Sazanov
 682 2015). The H⁺_{neg}/P_» coupling stoichiometry (3.7; **Fig. 1A**) is the sum of 2.7 H⁺_{neg} required by
 683 the F₁F₀-ATPase of vertebrate and most invertebrate species (Watt *et al.* 2010) and the proton
 684 balance in the translocation of ADP, ATP and P_i (**Fig. 1B**). Taken together, the mechanistic
 685 P_»/O₂ ratio is calculated at 5.4 and 3.3 for NADH- and succinate-linked respiration, respectively
 686 (Eq. 1). The corresponding classical P_»/O ratios (referring to the 2 electron reduction of 0.5 O₂)
 687 are 2.7 and 1.6 (Watt *et al.* 2010), in direct agreement with the measured P_»/O ratio for succinate
 688 of 1.58 ± 0.02 (Gnaiger *et al.* 2000).

689 The effective P_»/O₂ flux ratio ($Y_{P_{\gg}/O_2} = J_{P_{\gg}}/J_{kO_2}$) is diminished relative to the mechanistic
 690 P_»/O₂ ratio by intrinsic and extrinsic uncoupling and dyscoupling (**Fig. 3**). Such generalized
 691 uncoupling is different from switching to mitochondrial pathways that involve fewer than three
 692 proton pumps (‘coupling sites’: Complexes CI, CIII and CIV), bypassing CI through multiple
 693 electron entries into the Q-junction, or CIII and CIV through AOX (**Fig. 1**). Reprogramming of
 694 mitochondrial pathways may be considered as a switch of gears (changing the stoichiometry)
 695 rather than uncoupling (loosening the stoichiometry). In addition, Y_{P_{\gg}/O_2} depends on several
 696 experimental conditions of flux control, increasing as a hyperbolic function of [ADP] to a
 697 maximum value (Gnaiger 2001).

698 The net OXPHOS-capacity is calculated by subtracting *L* from *P* (**Fig. 5**). Then the net
 699 P_»/O₂ equals P_»/(*P*-*L*), wherein the dissipative LEAK component in the OXPHOS-state may
 700 be overestimated. This can be avoided by measuring LEAK-respiration in a state when the
 701 protonmotive force is adjusted to its slightly lower value in the OXPHOS-state—by titration of
 702 an ET inhibitor (Divakaruni and Brand 2011). Any turnover-dependent components of proton
 703 leak and slip, however, are underestimated under these conditions (Garlid *et al.* 1993). In
 704 general, it is inappropriate to use the term *ATP production* or *ATP turnover* for the difference
 705 of oxygen consumption measured in states *P* and *L*. The difference *P*-*L* is the upper limit of the
 706 part of OXPHOS-capacity that is freely available for ATP production (corrected for LEAK-
 707 respiration) and is fully coupled to phosphorylation with a maximum mechanistic stoichiometry
 708 (**Fig. 5**).

709 **Control and regulation:** The terms metabolic *control* and *regulation* are frequently used
 710 synonymously, but are distinguished in metabolic control analysis: ‘We could understand the
 711 regulation as the mechanism that occurs when a system maintains some variable constant over
 712 time, in spite of fluctuations in external conditions (homeostasis of the internal state). On the
 713 other hand, metabolic control is the power to change the state of the metabolism in response to

714 an external signal' (Fell 1997). Respiratory control may be induced by experimental control
 715 signals that *exert* an influence on: (1) ATP demand and ADP phosphorylation-rate; (2) fuel
 716 substrate composition, pathway competition; (3) available amounts of substrates and oxygen,
 717 *e.g.*, starvation and hypoxia; (4) the protonmotive force, redox states, flux–force relationships,
 718 coupling and efficiency; (5) Ca²⁺ and other ions including H⁺; (6) inhibitors, *e.g.*, nitric oxide
 719 or intermediary metabolites such as oxaloacetate; (7) signalling pathways and regulatory
 720 proteins, *e.g.*, insulin resistance, transcription factor hypoxia inducible factor 1. *Mechanisms* of
 721 respiratory control and regulation include adjustments of: (1) enzyme activities by allosteric
 722 mechanisms and phosphorylation; (2) enzyme content, concentrations of cofactors and
 723 conserved moieties—such as adenylates, nicotinamide adenine dinucleotide [NAD⁺/NADH],
 724 coenzyme Q, cytochrome *c*; (3) metabolic channeling by supercomplexes; and (4)
 725 mitochondrial density (enzyme concentrations and membrane area) and morphology (cristae
 726 folding, fission and fusion). Mitochondria are targeted directly by hormones, thereby affecting
 727 their energy metabolism (Lee *et al.* 2013; Gerö and Szabo 2016; Price and Dai 2016; Moreno
 728 *et al.* 2017). Evolutionary or acquired differences in the genetic and epigenetic basis of
 729 mitochondrial function (or dysfunction) between subjects and gene therapy; age; gender,
 730 biological sex, and hormone concentrations; life style including exercise and nutrition; and
 731 environmental issues including thermal, atmospheric, toxicological and pharmacological
 732 factors, exert an influence on all control mechanisms listed above. For reviews, see Brown
 733 1992; Gnaiger 1993a, 2009; 2014; Paradies *et al.* 2014; Morrow *et al.* 2017.

734 **Respiratory control and response:** Lack of control by a metabolic pathway, *e.g.*,
 735 phosphorylation-pathway, means that there will be no response to a variable activating it, *e.g.*,
 736 [ADP]. The reverse, however, is not true as the absence of a response to [ADP] does not exclude
 737 the phosphorylation-pathway from having some degree of control. The degree of control of a
 738 component of the OXPHOS-pathway on an output variable—such as oxygen flux, will in
 739 general be different from the degree of control on other outputs—such as phosphorylation-flux
 740 or proton leak flux. Therefore, it is necessary to be specific as to which input and output are
 741 under consideration (Fell 1997).

742 **Respiratory coupling control:** Respiratory control refers to the ability of mitochondria
 743 to adjust oxygen consumption in response to external control signals by engaging various
 744 mechanisms of control and regulation. Respiratory control is monitored in a mitochondrial
 745 preparation under conditions defined as respiratory states. When phosphorylation of ADP to
 746 ATP is stimulated or depressed, an increase or decrease is observed in electron flux linked to
 747 oxygen consumption in respiratory coupling states of intact mitochondria ('controlled states' in
 748 the classical terminology of bioenergetics). Alternatively, coupling of electron transfer with
 749 phosphorylation is disengaged by disruption of the integrity of the mtIM or by uncouplers,
 750 functioning like a clutch in a mechanical system. The corresponding coupling control state is
 751 characterized by high levels of oxygen consumption without control by phosphorylation
 752 ('uncontrolled state').

753 **ET-pathway control states** are obtained in mitochondrial preparations by depletion of
 754 endogenous substrates and addition to the mitochondrial respiration medium of fuel substrates
 755 (CHNO; 2[H] in **Fig. 2**) and specific inhibitors, activating selected mitochondrial catabolic
 756 pathways, *k* (**Fig. 1**). Coupling control states and pathway control states are complementary,
 757 since mitochondrial preparations depend on an exogenous supply of pathway-specific fuel
 758 substrates and oxygen (Gnaiger 2014).

759
 760 **2.3. Classical terminology for isolated mitochondria**

761 *'When a code is familiar enough, it ceases appearing like a code; one forgets that there*
 762 *is a decoding mechanism. The message is identical with its meaning'* (Hofstadter 1979).

763

764 Chance and Williams (1955; 1956) introduced five classical states of mitochondrial respiration
 765 and cytochrome redox states. **Table 3** shows a protocol with isolated mitochondria in a closed
 766 respirometric chamber, defining a sequence of respiratory states. States and rates are not
 767 specifically distinguished in this nomenclature.

768
 769 **Table 3. Metabolic states of mitochondria (Chance and**
 770 **Williams, 1956; Table V).**

State	[O ₂]	ADP level	Substrate Level	Respiration rate	Rate-limiting substance
1	>0	low	low	slow	ADP
2	>0	high	~0	slow	substrate
3	>0	high	high	fast	respiratory chain
4	>0	low	high	slow	ADP
5	0	high	high	0	oxygen

772
 773

774 **State 1** is obtained after addition of isolated mitochondria to air-saturated
 775 isoosmotic/isotonic respiration medium containing inorganic phosphate, but no fuel substrates
 776 and no adenylates, *i.e.*, AMP, ADP, ATP.

777 **State 2** is induced by addition of a ‘high’ concentration of ADP (typically 100 to 300
 778 μM), which stimulates respiration transiently on the basis of endogenous fuel substrates and
 779 phosphorylates only a small portion of the added ADP. State 2 is then obtained at a low
 780 respiratory activity limited by exhausted endogenous fuel substrate availability (**Table 3**). If
 781 addition of specific inhibitors of respiratory complexes—such as rotenone—does not cause a
 782 further decline of oxygen consumption, State 2 is equivalent to the state of residual oxygen
 783 consumption, ROX (See below.). If inhibition is observed, undefined endogenous fuel
 784 substrates are a confounding factor of pathway control, contributing to the effect of
 785 subsequently externally added substrates and inhibitors. In contrast to the original protocol, an
 786 alternative sequence of titration steps is frequently applied, in which the alternative ‘State 2’
 787 has an entirely different meaning, when this second state is induced by addition of fuel substrate
 788 without ADP (LEAK-state; in contrast to State 2 defined in **Table 1** as a ROX state), followed
 789 by addition of ADP.

790 **State 3** is the state stimulated by addition of fuel substrates while the ADP concentration
 791 is still high (**Table 3**) and supports coupled energy transformation through oxidative
 792 phosphorylation. ‘High ADP’ is a concentration of ADP specifically selected to allow the
 793 measurement of State 3 to State 4 transitions of isolated mitochondria in a closed respirometric
 794 chamber. Repeated ADP titration re-establishes State 3 at ‘high ADP’. Starting at oxygen
 795 concentrations near air-saturation (ca. 200 μM O₂ at sea level and 37 °C), the total ADP
 796 concentration added must be low enough (typically 100 to 300 μM) to allow phosphorylation
 797 to ATP at a coupled rate of oxygen consumption that does not lead to oxygen depletion during
 798 the transition to State 4. In contrast, kinetically-saturating ADP concentrations usually are 10-
 799 fold higher than ‘high ADP’, *e.g.*, 2.5 mM in isolated mitochondria. The abbreviation State 3u
 800 is occasionally used in bioenergetics, to indicate the state of respiration after titration of an
 801 uncoupler, without sufficient emphasis on the fundamental difference between OXPHOS-
 802 capacity (*well-coupled* with an *endogenous* uncoupled component) and ET-capacity
 803 (*noncoupled*).

804 **State 4** is a LEAK-state that is obtained only if the mitochondrial preparation is intact
 805 and well-coupled. Depletion of ADP by phosphorylation to ATP leads to a decline in the rate
 806 of oxygen consumption in the transition from State 3 to State 4. Under these conditions of State
 807 4, a maximum protonmotive force and high ATP/ADP ratio are maintained. For calculation of

808 P_{\gg}/O_2 ratios the gradual decline of Y_{P_{\gg}/O_2} towards diminishing [ADP] at State 4 must be taken
 809 into account (Gnaiger 2001). State 4 respiration, L_T (**Table 1**), reflects intrinsic proton leak and
 810 intrinsic ATP hydrolysis activity. Oxygen consumption in State 4 is an overestimation of
 811 LEAK-respiration if the contaminating ATP hydrolysis activity recycles some ATP to ADP,
 812 $J_{P_{\ll}}$, which stimulates respiration coupled to phosphorylation, $J_{P_{\gg}} > 0$. This can be tested by
 813 inhibition of the phosphorylation-pathway using oligomycin, ensuring that $J_{P_{\gg}} = 0$ (State 4o).
 814 Alternatively, sequential ADP titrations re-establish State 3, followed by State 3 to State 4
 815 transitions while sufficient oxygen is available. Anoxia may be reached, however, before
 816 exhaustion of ADP (State 5).

817 **State 5** is the state after exhaustion of oxygen in a closed respirometric chamber.
 818 Diffusion of oxygen from the surroundings into the aqueous solution may be a confounding
 819 factor preventing complete anoxia (Gnaiger 2001). Chance and Williams (1955) provide an
 820 alternative definition of State 5, which gives it the different meaning of ROX versus anoxia:
 821 ‘State 5 may be obtained by antimycin A treatment or by anaerobiosis’.

822 In **Table 3**, only States 3 and 4 (and ‘State 2’ in the alternative protocol: addition of fuel
 823 substrates without ADP; not included in the table) are coupling control states, with the
 824 restriction that O_2 flux in State 3 may be limited kinetically by non-saturating ADP
 825 concentrations (**Table 1**).

826
827

828 3. Normalization: fluxes and flows

829

830 3.1. Normalization: system or sample

831

832 The term *rate* is not sufficiently defined to be useful for a database (**Fig. 6**). The
 833 inconsistency of the meanings of rate becomes fully apparent when considering Galileo
 834 Galilei’s famous principle, that ‘bodies of different weight all fall at the same rate (have a
 835 constant acceleration)’ (Coopersmith 2010).

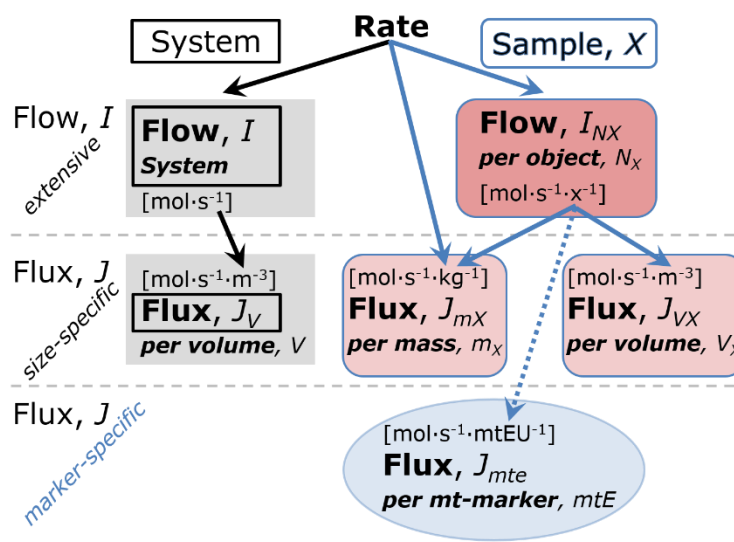
836

837 **Fig. 6. Different meanings of rate may lead to confusion, if the normalization is not sufficiently specified.** Results are frequently expressed as mass-specific flux, J_{mX} , per mg protein, dry or wet weight (mass). Cell volume, V_{cell} , may be used for normalization (volume-specific flux, J_{Vcell}), which must be clearly distinguished from flow per cell, I_{Ncell} , or flux, J_V , expressed for methodological reasons per volume of the measurement system. For details see **Table 4**.

852

853 **Flow per system, I :** In a generalization of electrical terms, flow as an extensive quantity (per system) is distinguished from flux as a size-specific quantity (per system size) (**Fig. 6**). Electric current is flow, I_{el} [$A \equiv C \cdot s^{-1}$] per system (extensive quantity). When dividing this extensive quantity by system size (cross-sectional area of a ‘wire’), a size-specific quantity is obtained, which is flux (current density), J_{el} [$A \cdot m^{-2} = C \cdot s^{-1} \cdot m^{-2}$].

858 **Extensive quantities:** An extensive quantity increases proportionally with system size.
 859 The magnitude of an extensive quantity is completely additive for non-interacting



860 subsystems—such as mass or flow expressed per defined system. The magnitude of these
861 quantities depends on the extent or size of the system (Cohen *et al.* 2008).

862 **Size-specific quantities:** ‘The adjective *specific* before the name of an extensive quantity
863 is often used to mean *divided by mass*’ (Cohen *et al.* 2008). In this system-paradigm, mass-
864 specific flux is flow divided by mass of the *system* (the total mass of everything within the
865 measuring chamber). A mass-specific quantity is independent of the extent of non-interacting
866 homogenous subsystems. Tissue-specific quantities (related to the *sample* in contrast to the
867 *system*) are of fundamental interest in comparative mitochondrial physiology, where *specific*
868 refers to the *type of the sample* rather than *mass of the system*. The term *specific*, therefore, must
869 be clarified; *sample-specific*, *e.g.*, muscle mass-specific normalization, is distinguished from
870 *system-specific* (mass or volume) quantities (**Fig. 6**).

871

872 **Box 2: Metabolic fluxes and flows: vectorial and scalar**

873

874 Fluxes are *vectors*, if they have *spatial* direction in addition to magnitude. A vector flux
875 (surface-density of flow) is expressed per unit cross-sectional area, A [m^2], perpendicular to the
876 direction of flux. *Flows* are defined as extensive quantities of the *system*, as vector or scalar
877 flow, I or I [$\text{mol}\cdot\text{s}^{-1}$], respectively, then the corresponding vector and scalar *fluxes* are $J = I\cdot A^{-1}$
878 [$\text{mol}\cdot\text{s}^{-1}\cdot\text{m}^{-2}$] and $J = I\cdot V^{-1}$ [$\text{mol}\cdot\text{s}^{-1}\cdot\text{m}^{-3}$], respectively, expressing flux as an area-specific vector
879 or volume-specific scalar quantity. We suggest to define: (1) *vectorial* fluxes, which analyze
880 translocations in continuous systems as functions of gradients; (2) *vectorial* fluxes, which
881 describe translocations in discontinuous systems and are restricted to information on
882 compartmental differences (**Fig. 2**, transmembrane proton flux); and (3) *scalar* fluxes, which
883 are transformations in a homogenous system (**Fig. 2**, catabolic O_2 flux, J_{KO_2} [$\text{mol}\cdot\text{s}^{-1}\cdot\text{m}^{-3}$]).

884 Vectorial transmembrane proton fluxes, $J_{\text{mH}^+\text{pos}}$ and $J_{\text{mH}^+\text{neg}}$, are analyzed in a
885 heterogenous compartmental system as a quantity with *directional* but not *spatial* information.
886 Translocation of protons across the mtIM has a defined direction, either from the negative
887 compartment (matrix space; negative, neg–compartment) to the positive compartment (inter-
888 membrane space; positive, pos–compartment) or *vice versa* (**Fig. 2**). The arrows defining the
889 direction of the translocation between the two compartments may point upwards or downwards,
890 right or left, without any implication that these are actual directions in space. The pos–
891 compartment is neither above nor below the neg–compartment in a spatial sense, but can be
892 visualized arbitrarily in a figure in the upper position (**Fig. 2**). In general, the *compartmental*
893 *direction* of vectorial translocation from the neg–compartment to the pos–compartment is
894 defined by assigning the initial and final state as *ergodynamic compartments*, $\text{H}^+_{\text{neg}} \rightarrow \text{H}^+_{\text{pos}}$ Or
895 $0 = -1 \text{H}^+_{\text{neg}} + 1 \text{H}^+_{\text{pos}}$, related to work (erg = work) that must be performed to lift the proton from
896 a lower to a higher electrochemical potential or from the lower to the higher ergodynamic
897 compartment (Gnaiger 1993b).

898 In direct analogy to *vectorial* translocation, the direction of a *scalar* chemical reaction, A
899 $\rightarrow B$ or $0 = -1 A + 1 B$, is defined by assigning substrates and products, A and B, as ergodynamic
900 compartments. O_2 is defined as a substrate in respiratory O_2 consumption, which together with
901 the fuel substrates comprises the substrate compartment of the catabolic reaction (**Fig. 2**).
902 Volume-specific scalar O_2 flux is coupled to vectorial translocation, yielding the $\text{H}^+_{\text{pos}}/\text{O}_2$ ratio
903 (**Fig. 1**).

904

905 3.2. Normalization for system-size: flux per chamber volume

906

907 **System-specific flux, J :** The experimental system (the experimental chamber) is part of
908 the measurement apparatus, separated from the environment as an isolated, closed, open,
909 isothermal or non-isothermal system (**Table 4**). On another level, we distinguish between (1)
910 the *system* with volume V and mass m defined by the system boundaries, and (2) the *sample* or

911 *objects* with volume V_X and mass m_X which are enclosed in the experimental chamber (**Fig. 6**).
 912 Metabolic O_2 flow per object, I_{X,O_2} , increases as the mass of the object is increased. Object mass-
 913 specific O_2 flux, J_{mX,O_2} should be independent of the mass of the object studied in the instrument
 914 chamber, but system volume-specific O_2 flux, J_{V,O_2} (per volume of the instrument chamber),
 915 should increase in direct proportion to the mass of the object in the chamber. J_{V,O_2} depends on
 916 mass-concentration of the sample in the chamber, but should be independent of the chamber
 917 (system) volume. There are practical limitations to increase the mass-concentration of the
 918 sample in the chamber, when one is concerned about crowding effects and instrumental time
 919 resolution.

920 When the reactor volume does not change during the reaction, which is typical for liquid
 921 phase reactions, the volume-specific flux of a chemical reaction r is the time derivative of the
 922 advancement of the reaction per unit volume, $J_{V,rB} = d_{r\zeta_B}/dt \cdot V^{-1}$ [(mol·s⁻¹)·L⁻¹]. The rate of
 923 concentration change is dc_B/dt [(mol·L⁻¹)·s⁻¹], where concentration is $c_B = n_B/V$. There is a
 924 difference between (1) J_{V,rO_2} [mol·s⁻¹·L⁻¹] and (2) rate of concentration change [mol·L⁻¹·s⁻¹].
 925 These merge to a single expression only in closed systems. In open systems, external fluxes
 926 (such as O_2 supply) are distinguished from internal transformations (metabolic flux, O_2
 927 consumption). In a closed system, external flows of all substances are zero and O_2 consumption
 928 (internal flow of catabolic reactions k), I_{kO_2} [pmol·s⁻¹], causes a decline of the amount of O_2 in
 929 the system, n_{O_2} [nmol]. Normalization of these quantities for the volume of the system, V [L \equiv
 930 dm³], yields volume-specific O_2 flux, $J_{V,kO_2} = I_{kO_2}/V$ [nmol·s⁻¹·L⁻¹], and O_2 concentration, $[O_2]$
 931 or $c_{O_2} = n_{O_2}/V$ [μ mol·L⁻¹ = μ M = nmol·mL⁻¹]. Instrumental background O_2 flux is due to external
 932 flux into a non-ideal closed respirometer; then total volume-specific flux has to be corrected for
 933 instrumental background O_2 flux— O_2 diffusion into or out of the instrumental chamber. J_{V,kO_2}
 934 is relevant mainly for methodological reasons and should be compared with the accuracy of
 935 instrumental resolution of background-corrected flux, e.g., ± 1 nmol·s⁻¹·L⁻¹ (Gnaiger 2001).
 936 ‘Metabolic’ or catabolic indicates O_2 flux, J_{kO_2} , corrected for: (1) instrumental background O_2
 937 flux; (2) chemical background O_2 flux due to autoxidation of chemical components added to
 938 the incubation medium; and (3) Rox for O_2 -consuming side reactions unrelated to the catabolic
 939 pathway k .

940 3.3. Normalization: per sample

941 The challenges of measuring mitochondrial respiratory flux are matched by those of
 942 normalization. Application of common and defined units is required for direct transfer of
 943 reported results into a database. The second [s] is the *SI* unit for the base quantity *time*. It is also
 944 the standard time-unit used in solution chemical kinetics. A rate may be considered as the
 945 numerator and normalization as the complementary denominator, which are tightly linked in
 946 reporting the measurements in a format commensurate with the requirements of a database.
 947 Normalization (**Table 4**) is guided by physicochemical principles, methodological
 948 considerations, and conceptual strategies (**Fig. 7**).

949 **Sample concentration, C_{mX} :** Normalization for sample concentration is required to
 950 report respiratory data. Considering a tissue or cells as the sample, X , the sample mass is m_X
 951 [mg] from which a mitochondrial preparation is obtained. m_X is frequently measured as wet or
 952 dry weight, W_w or W_d [mg], or as amount of tissue or cell protein, $m_{Protein}$. In the case of
 953 permeabilized tissues, cells, and homogenates, the sample concentration, $C_{mX} = m_X/V$ [mg·mL⁻¹
 954 = g·L⁻¹], is simply the mass of the subsample of tissue that is transferred into the instrument
 955 chamber.

956 **Mass-specific flux, J_{mX,O_2} :** Mass-specific flux is obtained by expressing respiration per
 957 mass of sample, m_X [mg]. X is the type of sample—tissue homogenate, permeabilized fibres or
 958 cells. Volume-specific flux is divided by mass concentration of X , $J_{mX,O_2} = J_{V,O_2}/C_{mX}$; or flow
 959 per cell is divided by mass per cell, $J_{mcell,O_2} = I_{cell,O_2}/M_{cell}$. If mass-specific O_2 flux is constant
 960
 961

962 and independent of sample size (expressed as mass), then there is no interaction between the
 963 subsystems. A 1.5 mg and a 3.0 mg muscle sample respire at identical mass-specific flux.
 964 Mass-specific O₂ flux, however, may change with the mass of a tissue sample, cells or isolated
 965 mitochondria in the measuring chamber, in which the nature of the interaction becomes an issue.
 966 Therefore, cell density must be optimization, particularly in experiments carried out in wells,
 967 considering the confluency of the cell monolayer or clumps of cells (Salabei *et al.* 2014).
 968

969

Table 4. Sample concentrations and normalization of flux.

Expression	Symbol	Definition	Unit	Notes
Sample				
identity of sample	X	object: cell, tissue, animal, patient		
number of sample entities X	N_X	number of objects	x	
mass of sample X	m_X		kg	1
mass of object X	M_X	$M_X = m_X \cdot N_X^{-1}$	kg·x ⁻¹	1
Mitochondria				
Mitochondria	mt	$X = \text{mt}$		
amount of mt-elements	mtE	quantity of mt-marker	mtEU	
Concentrations				
object number concentration	C_{NX}	$C_{NX} = N_X \cdot V^{-1}$	x·m ⁻³	2
sample mass concentration	C_{mX}	$C_{mX} = m_X \cdot V^{-1}$	kg·m ⁻³	
mitochondrial concentration	C_{mtE}	$C_{mtE} = mtE \cdot V^{-1}$	mtEU·m ⁻³	3
specific mitochondrial density	D_{mtE}	$D_{mtE} = mtE \cdot m_X^{-1}$	mtEU·kg ⁻¹	4
mitochondrial content, mtE per object X	mtE_X	$mtE_X = mtE \cdot N_X^{-1}$	mtEU·x ⁻¹	5
O₂ flow and flux				
flow, system	I_{O_2}	internal flow	mol·s ⁻¹	6
volume-specific flux	J_{V,O_2}	$J_{V,O_2} = I_{O_2} \cdot V^{-1}$	mol·s ⁻¹ ·m ⁻³	7
flow per object X	I_{X,O_2}	$I_{X,O_2} = J_{V,O_2} \cdot C_{NX}^{-1}$	mol·s ⁻¹ ·x ⁻¹	8
mass-specific flux	J_{mX,O_2}	$J_{mX,O_2} = J_{V,O_2} \cdot C_{mX}^{-1}$	mol·s ⁻¹ ·kg ⁻¹	9
mitochondria-specific flux	J_{mtE,O_2}	$J_{mtE,O_2} = J_{V,O_2} \cdot C_{mtE}^{-1}$	mol·s ⁻¹ ·mtEU ⁻¹	10

- 971 1 The SI prefix k is used for the SI base unit of mass (kg = 1,000 g). In praxis, various SI prefixes are
 972 used for convenience, to make numbers easily readable, e.g., 1 mg tissue, cell or mitochondrial mass
 973 instead of 0.000001 kg.
- 974 2 In case sample $X = \text{cells}$, the object number concentration is $C_{N_{\text{cell}}} = N_{\text{cell}} \cdot V^{-1}$, and volume may be
 975 expressed in [dm³ ≡ L] or [cm³ = mL]. See **Table 5** for different object types.
- 976 3 mt-concentration is an experimental variable, dependent on sample concentration: (1) $C_{mtE} = mtE \cdot V^{-1}$;
 977 (2) $C_{mtE} = mtE_X \cdot C_{NX}$; (3) $C_{mtE} = C_{mX} \cdot D_{mtE}$.
- 978 4 If the amount of mitochondria, mtE , is expressed as mitochondrial mass, then D_{mtE} is the mass
 979 fraction of mitochondria in the sample. If mtE is expressed as mitochondrial volume, V_{mt} , and the
 980 mass of sample, m_X , is replaced by volume of sample, V_X , then D_{mtE} is the volume fraction of
 981 mitochondria in the sample.
- 982 5 $mtE_X = mtE \cdot N_X^{-1} = C_{mtE} \cdot C_{NX}^{-1}$.
- 983 6 O₂ can be replaced by other chemicals B to study different reactions, e.g., ATP, H₂O₂, or
 984 compartmental translocations, e.g., Ca²⁺.
- 985 7 I_{O_2} and V are defined per instrument chamber as a system of constant volume (and constant
 986 temperature), which may be closed or open. I_{O_2} is abbreviated for $I_{O_2,r}$ —the metabolic or internal O₂
 987 flow of the chemical reaction r in which O₂ is consumed—hence the negative stoichiometric number,
 988 $\nu_{O_2} = -1$. $I_{O_2,r} = d_n n_{O_2} / dt \cdot \nu_{O_2}^{-1}$. If r includes all chemical reactions in which O₂ participates, then $d_r n_{O_2} = dn_{O_2}$
 989 $- d_e n_{O_2}$, where dn_{O_2} is the change in the amount of O₂ in the instrument chamber and $d_e n_{O_2}$ is the

- 990 amount of O₂ added externally to the system. At steady state, by definition $dn_{O_2} = 0$, hence $d_r n_{O_2} = -$
 991 $d_e n_{O_2}$.
 992 8 J_{V,O_2} is an experimental variable, expressed per volume of the instrument chamber.
 993 9 I_{X,O_2} is a physiological variable, depending on the size of entity X .
 994 10 There are many ways to normalize for a mitochondrial marker, that are used in different experimental
 995 approaches: (1) $J_{mtE,O_2} = J_{V,O_2} \cdot C_{mtE}^{-1}$; (2) $J_{mtE,O_2} = J_{V,O_2} \cdot C_{mX}^{-1} \cdot D_{mtE}^{-1} = J_{mX,O_2} \cdot D_{mtE}^{-1}$; (3) $J_{mtE,O_2} =$
 996 $J_{V,O_2} \cdot C_{NX}^{-1} \cdot mtE_X^{-1} = I_{X,O_2} \cdot mtE_X^{-1}$; (4) $J_{mtE,O_2} = I_{O_2} \cdot mtE^{-1}$. The mt-elemental unit [mtEU] varies between
 997 different mt-markers.
 998
 999

Table 5. Sample types, X, abbreviations, and quantification.

Identity of sample	X	N_X	Mass ^a	Volume	mt-Marker
mitochondrial preparation	mtprep	[x]	[kg]	[m ³]	[mtEU]
isolated mitochondria	imt		m_{mt}	V_{mt}	mtE
tissue homogenate	thom		m_{thom}		mtE_{thom}
permeabilized tissue	pti		m_{pti}		mtE_{pti}
permeabilized fibre	pfi		m_{pfi}		mtE_{pfi}
permeabilized cell	pce	N_{pce}	M_{pce}	V_{pce}	mtE_{pce}
intact cell	ce	N_{ce}	M_{ce}	V_{ce}	mtE_{ce}
Organism	org	N_{org}	M_{org}	V_{org}	

^a Instead of mass, frequently the wet weight or dry weight is stated, W_w or W_d .
 m_X is mass of the sample [kg], M_X is mass of the object [kg·x⁻¹].

Number concentration, C_{NX} : C_{NX} is the experimental *number concentration* of sample X . In the case of cells or animals, *e.g.*, nematodes, $C_{NX} = N_X/V$ [x·L⁻¹], where N_X is the number of cells or organisms in the chamber (**Table 4**).

Flow per object, I_{X,O_2} : A special case of normalization is encountered in respiratory studies with permeabilized (or intact) cells. If respiration is expressed per cell, the O₂ flow per measurement system is replaced by the O₂ flow per cell, I_{cell,O_2} (**Table 4**). O₂ flow can be calculated from volume-specific O₂ flux, J_{V,O_2} [nmol·s⁻¹·L⁻¹] (per V of the measurement chamber [L]), divided by the number concentration of cells, $C_{Nce} = N_{ce}/V$ [cell·L⁻¹], where N_{ce} is the number of cells in the chamber. Cellular O₂ flow can be compared between cells of identical size. To take into account changes and differences in cell size, normalization is required to obtain cell size-specific or mitochondrial marker-specific O₂ flux (Renner *et al.* 2003).

The complexity changes when the sample is a whole organism studied as an experimental model. The scaling law in respiratory physiology reveals a strong interaction of O₂ consumption and individual body mass of an organism, since *basal* metabolic rate (flow) does not increase linearly with body mass, whereas *maximum* mass-specific O₂ flux, \dot{V}_{O_2max} or \dot{V}_{O_2peak} , is approximately constant across a large range of individual body mass (Weibel and Hoppeler 2005), with individuals, breeds, and species deviating substantially from this relationship. \dot{V}_{O_2peak} of human endurance athletes is 60 to 80 mL O₂·min⁻¹·kg⁻¹ body mass, converted to J_{M,O_2peak} of 45 to 60 nmol·s⁻¹·g⁻¹ (Gnaiger 2014; **Table 6**).

3.4. Normalization for mitochondrial content

Tissues can contain multiple cell populations that may have distinct mitochondrial subtypes. Mitochondria undergo dynamic fission and fusion cycles, and can exist in multiple stages and sizes which may be altered by a range of factors. The isolation of mitochondria (often achieved through differential centrifugation) can therefore yield a subsample of the mitochondrial types present in a tissue, depending on isolation protocols utilized (*e.g.*, centrifugation speed). This possible bias should be taken into account when planning experiments using isolated mitochondria. Different sizes of mitochondria are enriched at specific centrifugation speeds, which is used for isolation of mitochondrial subpopulations.

1033 Part of the mitochondrial content of a tissue is lost during preparation of isolated
 1034 mitochondria. The fraction of mitochondria in the isolate is expressed as mitochondrial
 1035 recovery. At a high mitochondrial recovery the sample of isolated mitochondria is more
 1036 representative of the total mitochondrial population than in preparations characterized by low
 1037 recovery. Determination of the mitochondrial recovery and yield is based on measurement of
 1038 the concentration of a mitochondrial marker in the tissue homogenate, $C_{mtE,thom}$, which
 1039 simultaneously provides information on the specific mitochondrial density in the sample.

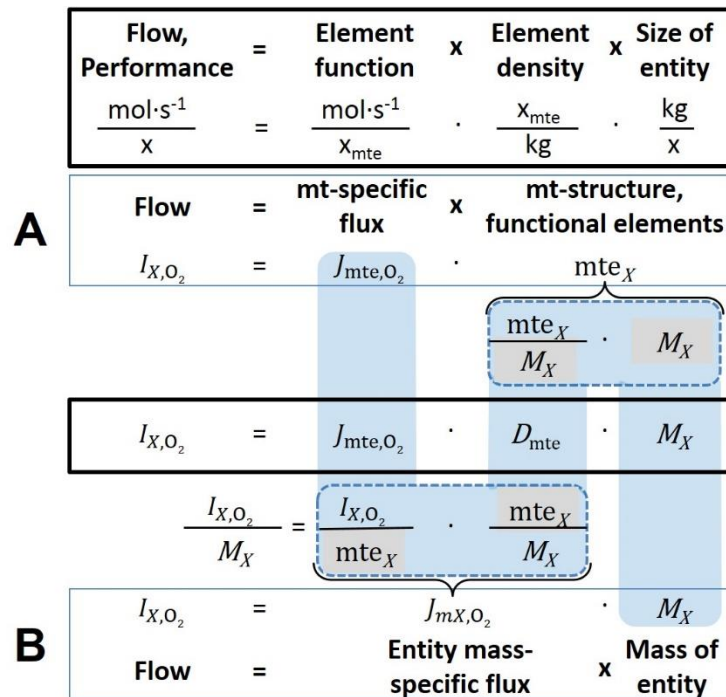
1040 Normalization is a problematic subject; it is essential to consider the question of the study.
 1041 If the study aims at comparing tissue performance—such as the effects of a treatment on a
 1042 specific tissue, then normalization can be successful, using tissue mass or protein content, for
 1043 example. However, if the aim is to find differences on mitochondrial function independent of
 1044 mitochondrial density (**Table 4**), then normalization to a mitochondrial marker is imperative
 1045 (**Fig. 7**). One cannot assume that quantitative changes in various markers—such as
 1046 mitochondrial proteins—necessarily occur in parallel with one another. It should be established
 1047 that the marker chosen is not selectively altered by the performed treatment. In conclusion, the
 1048 normalization must reflect the question under investigation to reach a satisfying answer. On the
 1049 other hand, the goal of comparing results across projects and institutions requires
 1050 standardization on normalization for entry into a databank.

1051 **Mitochondrial concentration, C_{mtE} , and mitochondrial markers:** Mitochondrial
 1052 concentration in the tissue and the measurement chamber are quantified as (1) a physiological
 1053 output that is the result of mitochondrial biogenesis and degradation, and (2) a quantity for
 1054 normalization in functional analyses. Mitochondrial organelles comprise a dynamic cellular
 1055 reticulum in various states of fusion and fission. Hence, the definition of an "amount" of
 1056 mitochondria is often misconceived: mitochondria cannot be counted reliably as a number of
 1057 occurring elements. Therefore, quantification of the "amount" of mitochondria depends on the
 1058 measurement of chosen mitochondrial markers. 'Mitochondria are the structural and functional
 1059 elemental units of cell respiration' (Gnaiger 2014). The quantity of a mitochondrial marker can
 1060 reflect the amount of *mitochondrial elements*, mtE , expressed in various mitochondrial
 1061 elemental units [mtEU] specific for each measured mt-marker (**Table 4**). However, since
 1062 mitochondrial quality may change in response to stimuli—particularly in mitochondrial
 1063 dysfunction and after exercise training (Pesta *et al.* 2011; Campos *et al.* 2017)—some markers
 1064 can vary while others are unchanged: (1) Mitochondrial volume and membrane area are
 1065 structural markers, whereas mitochondrial protein mass is frequently used as a marker for
 1066 isolated mitochondria. (2) Molecular and enzymatic mitochondrial markers (amounts or
 1067 activities) can be selected as matrix markers, *e.g.*, citrate synthase activity, mtDNA; mtIM-
 1068 markers, *e.g.*, cytochrome *c* oxidase activity, aa_3 content, cardiolipin, or mtOM-markers, *e.g.*,
 1069 TOM20. (3) Extending the measurement of mitochondrial marker enzyme activity to
 1070 mitochondrial pathway capacity, ET- or OXPHOS-capacity can be considered as an integrative
 1071 functional mitochondrial marker.

1072 Depending on the type of mitochondrial marker, the mitochondrial elements, mtE , are
 1073 expressed in marker-specific units. It is recommended to distinguish *experimental*
 1074 *mitochondrial concentration*, $C_{mtE} = mtE/V$ and *physiological mitochondrial density*, $D_{mtE} =$
 1075 mtE/m_X . Then mitochondrial density is the amount of mitochondrial elements per mass of tissue,
 1076 which is a biological variable (**Fig. 7**). The experimental variable is mitochondrial density
 1077 multiplied by sample mass concentration in the measuring chamber, $C_{mtE} = D_{mtE} \cdot C_{mX}$, or
 1078 mitochondrial content multiplied by sample number concentration, $C_{mtE} = mtE_X \cdot C_{NX}$ (**Table 4**).

1079 **Mitochondria-specific flux, J_{mtE,O_2} :** Volume-specific metabolic O_2 flux depends on: (1)
 1080 the sample concentration in the volume of the instrument chamber, C_{mX} , or C_{NX} ; (2) the
 1081 mitochondrial density in the sample, $D_{mtE} = mtE/m_X$ or $mtE_X = mtE/N_X$; and (3) the specific
 1082 mitochondrial activity or performance per elemental mitochondrial unit, $J_{mtE,O_2} = J_{V,O_2}/C_{mtE}$

1083 [mol·s⁻¹·mtEU⁻¹] (Table 4). Obviously, the numerical results for J_{mtE,O_2} vary with the type of
 1084 mitochondrial marker chosen for measurement of mtE and $C_{mtE} = mtE/V$ [mtEU·m⁻³].
 1085



1086 **Fig. 7. Structure-function analysis of performance of an organism, organ or tissue, or a**
 1087 **cell (sample entity, X). O₂ flow, I_{X,O_2} , is the product of performance per functional element**
 1088 **(element function, mitochondria-specific flux), element density (mitochondrial density,**
 1089 **D_{mtE}), and size of entity X (mass, M_X). (A) Structured analysis: performance is the product of**
 1090 **mitochondrial function (mt-specific flux) and structure (functional elements; D_{mtE} times mass**
 1091 **of X). (B) Unstructured analysis: performance is the product of entity mass-specific flux, J_{mX,O_2}**
 1092 **$= I_{X,O_2}/M_X = I_{O_2}/m_X$ [mol·s⁻¹·kg⁻¹] and size of entity, expressed as mass of X; $M_X = m_X \cdot N_X^{-1}$**
 1093 **[kg·X⁻¹]. See Table 4 for further explanation of quantities and units. Modified from Gnaiger**
 1094 **(2014).**
 1095
 1096

1097 3.5. Evaluation of mitochondrial markers

1098
 1099 Different methods are implicated in the quantification of mitochondrial markers and have
 1100 different strengths. Some problems are common for all mitochondrial markers, mtE : (1)
 1101 Accuracy of measurement is crucial, since even a highly accurate and reproducible
 1102 measurement of O₂ flux results in an inaccurate and noisy expression normalized for a biased
 1103 and noisy measurement of a mitochondrial marker. This problem is acute in mitochondrial
 1104 respiration because the denominators used (the mitochondrial markers) are often small moieties
 1105 of which accurate and precise determination is difficult. This problem can be avoided when O₂
 1106 fluxes measured in substrate-uncoupler-inhibitor titration protocols are normalized for flux in
 1107 a defined respiratory reference state, which is used as an *internal* marker and yields flux control
 1108 ratios, *FCRs*. *FCRs* are independent of any *externally* measured markers and, therefore, are
 1109 statistically robust, considering the limitations of ratios in general (Jasienski and Bazzaz 1999).
 1110 *FCRs* indicate qualitative changes of mitochondrial respiratory control, with highest
 1111 quantitative resolution, separating the effect of mitochondrial density or concentration on J_{mX,O_2}
 1112 and I_{X,O_2} from that of function per elemental mitochondrial marker, J_{mtE,O_2} (Pesta *et al.* 2011;
 1113 Gnaiger 2014). (2) If mitochondrial quality does not change and only the amount of
 1114 mitochondria varies as a determinant of mass-specific flux, any marker is equally qualified in
 1115 principle; then in practice selection of the optimum marker depends only on the accuracy and

1116 precision of measurement of the mitochondrial marker. (3) If mitochondrial flux control ratios
1117 change, then there may not be any best mitochondrial marker. In general, measurement of
1118 multiple mitochondrial markers enables a comparison and evaluation of normalization for a
1119 variety of mitochondrial markers. Particularly during postnatal development, the activity of
1120 marker enzymes—such as cytochrome *c* oxidase and citrate synthase—follows different time
1121 courses (Drahota *et al.* 2004). Evaluation of mitochondrial markers in healthy controls is
1122 insufficient for providing guidelines for application in the diagnosis of pathological states and
1123 specific treatments.

1124 In line with the concept of the respiratory control ratio (Chance and Williams 1955a), the
1125 most readily used normalization is that of flux control ratios and flux control factors (Gnaiger
1126 2014). Selection of the state of maximum flux in a protocol as the reference state has the
1127 advantages of: (1) internal normalization; (2) statistical linearization of the response in the range
1128 of 0 to 1; and (3) consideration of maximum flux for integrating a large number of elemental
1129 steps in the OXPHOS- or ET-pathways. This reduces the risk of selecting a functional marker
1130 that is specifically altered by the treatment or pathology, yet increases the chance that the highly
1131 integrative pathway is disproportionately affected, *e.g.*, the OXPHOS- rather than ET-pathway
1132 in case of an enzymatic defect in the phosphorylation-pathway. In this case, additional
1133 information can be obtained by reporting flux control ratios based on a reference state which
1134 indicates stable tissue-mass specific flux. Stereological determination of mitochondrial content
1135 via two-dimensional transmission electron microscopy can have limitations due to the dynamics
1136 of mitochondrial size (Meinild Lundby *et al.* 2017). Accurate determination of three-
1137 dimensional volume by two-dimensional microscopy can be both time consuming and
1138 statistically challenging (Larsen *et al.* 2012).

1139 The validity of using mitochondrial marker enzymes (citrate synthase activity, Complex
1140 I–IV amount or activity) for normalization of flux is limited in part by the same factors that
1141 apply to flux control ratios. Strong correlations between various mitochondrial markers and
1142 citrate synthase activity (Reichmann *et al.* 1985; Boushel *et al.* 2007; Mogensen *et al.* 2007)
1143 are expected in a specific tissue of healthy subjects and in disease states not specifically
1144 targeting citrate synthase. Citrate synthase activity is acutely modifiable by exercise
1145 (Tonkonogi *et al.* 1997; Leek *et al.* 2001). Evaluation of mitochondrial markers related to a
1146 selected age and sex cohort cannot be extrapolated to provide recommendations for
1147 normalization in respirometric diagnosis of disease, in different states of development and
1148 ageing, different cell types, tissues, and species. mtDNA normalized to nDNA via qPCR is
1149 correlated to functional mitochondrial markers including OXPHOS- and ET-capacity in some
1150 cases (Puntschart *et al.* 1995; Wang *et al.* 1999; Menshikova *et al.* 2006; Boushel *et al.* 2007),
1151 but lack of such correlations have been reported (Menshikova *et al.* 2005; Schultz and Wiesner
1152 2000; Pesta *et al.* 2011). Several studies indicate a strong correlation between cardiolipin
1153 content and increase in mitochondrial function with exercise (Menshikova *et al.* 2005;
1154 Menshikova *et al.* 2007; Larsen *et al.* 2012; Faber *et al.* 2014), but its use as a general
1155 mitochondrial biomarker in disease remains questionable.

1156

1157 3.6. Conversion: units

1158

1159 Many different units have been used to report the rate of oxygen consumption, OCR
1160 (**Table 6**). *SI* base units provide the common reference to introduce the theoretical principles
1161 (**Fig. 6**), and are used with appropriately chosen *SI* prefixes to express numerical data in the
1162 most practical format, with an effort towards unification within specific areas of application
1163 (**Table 7**). Reporting data in *SI* units—including the mole [mol], coulomb [C], joule [J], and
1164 second [s]—should be encouraged, particularly by journals which propose the use of *SI* units.

1165

1166
1167
1168
1169**Table 6. Conversion of various units used in respirometry and ergometry.** e^- is the number of electrons or reducing equivalents. z_B is the charge number of entity B.

1 Unit	x	Multiplication factor	SI-unit	Note
ng.atom O \cdot s $^{-1}$	(2 e $^-$)	0.5	nmol O $_2$ \cdot s $^{-1}$	
ng.atom O \cdot min $^{-1}$	(2 e $^-$)	8.33	pmol O $_2$ \cdot s $^{-1}$	
natom O \cdot min $^{-1}$	(2 e $^-$)	8.33	pmol O $_2$ \cdot s $^{-1}$	
nmol O $_2$ \cdot min $^{-1}$	(4 e $^-$)	16.67	pmol O $_2$ \cdot s $^{-1}$	
nmol O $_2$ \cdot h $^{-1}$	(4 e $^-$)	0.2778	pmol O $_2$ \cdot s $^{-1}$	
mL O $_2$ \cdot min $^{-1}$ at STPD ^a		0.744	μ mol O $_2$ \cdot s $^{-1}$	1
W = J/s at -470 kJ/mol O $_2$		-2.128	μ mol O $_2$ \cdot s $^{-1}$	
mA = mC \cdot s $^{-1}$	($z_{H^+} = 1$)	10.36	nmol H $^+$ \cdot s $^{-1}$	2
mA = mC \cdot s $^{-1}$	($z_{O_2} = 4$)	2.59	nmol O $_2$ \cdot s $^{-1}$	2
nmol H $^+$ \cdot s $^{-1}$	($z_{H^+} = 1$)	0.09649	mA	3
nmol O $_2$ \cdot s $^{-1}$	($z_{O_2} = 4$)	0.38594	mA	3

1170
1171
1172
1173
1174
1175
1176
1177
1178
1179

- 1 At standard temperature and pressure dry (STPD: 0 °C = 273.15 K and 1 atm = 101.325 kPa = 760 mmHg), the molar volume of an ideal gas, V_m , and V_{m,O_2} is 22.414 and 22.392 L \cdot mol $^{-1}$, respectively. Rounded to three decimal places, both values yield the conversion factor of 0.744. For comparison at NTPD (20 °C), V_{m,O_2} is 24.038 L \cdot mol $^{-1}$. Note that the SI standard pressure is 100 kPa.
- 2 The multiplication factor is $10^6/(z_B \cdot F)$.
- 3 The multiplication factor is $z_B \cdot F/10^6$.

Table 7. Conversion of units with preservation of numerical values.

Name	Frequently used unit	Equivalent unit	Note
volume-specific flux, J_{V,O_2}	pmol \cdot s $^{-1}$ \cdot mL $^{-1}$	nmol \cdot s $^{-1}$ \cdot L $^{-1}$	1
	nmol \cdot s $^{-1}$ \cdot L $^{-1}$	mol \cdot s $^{-1}$ \cdot m $^{-3}$	
cell-specific flow, I_{O_2}	pmol \cdot s $^{-1}$ \cdot 10 $^{-6}$ cells	amol \cdot s $^{-1}$ \cdot cell $^{-1}$	2
	pmol \cdot s $^{-1}$ \cdot 10 $^{-9}$ cells	zmol \cdot s $^{-1}$ \cdot cell $^{-1}$	3
cell number concentration, C_{Nce}	10 6 cells \cdot mL $^{-1}$	10 9 cells \cdot L $^{-1}$	
mitochondrial protein concentration, C_{mtE}	0.1 mg \cdot mL $^{-1}$	0.1 g \cdot L $^{-1}$	
mass-specific flux, J_{m,O_2}	pmol \cdot s $^{-1}$ \cdot mg $^{-1}$	nmol \cdot s $^{-1}$ \cdot g $^{-1}$	4
catabolic power, P_k	μ W \cdot 10 $^{-6}$ cells	pW \cdot cell $^{-1}$	1
Volume	1,000 L	m 3 (1,000 kg)	
	L	dm 3 (kg)	
	mL	cm 3 (g)	
	μ L	mm 3 (mg)	
	fL	μ m 3 (pg)	5
amount of substance concentration	M = mol \cdot L $^{-1}$	mol \cdot dm $^{-3}$	

1180
1181
1182
1183
1184

- 1 pmol: picomole = 10 $^{-12}$ mol
- 2 amol: attomole = 10 $^{-18}$ mol
- 3 zmol: zeptomole = 10 $^{-21}$ mol
- 4 nmol: nanomole = 10 $^{-9}$ mol
- 5 fL: femtolitre = 10 $^{-15}$ L

1185 Although volume is expressed as m^3 using the *SI* base unit, the litre [dm^3] is a
 1186 conventional unit of volume for concentration and is used for most solution chemical kinetics.
 1187 If one multiplies $I_{\text{cell},\text{O}_2}$ by $C_{N_{\text{cell}}}$, then the result will not only be the amount of O_2 [mol]
 1188 consumed per time [s^{-1}] in one litre [L^{-1}], but also the change in the concentration of oxygen per
 1189 second (for any volume of an ideally closed system). This is ideal for kinetic modeling as it
 1190 blends with chemical rate equations where concentrations are typically expressed in $\text{mol}\cdot\text{L}^{-1}$
 1191 (Wagner *et al.* 2011). In studies of multinuclear cells—such as differentiated skeletal muscle
 1192 cells—it is easy to determine the number of nuclei but not the total number of cells. A
 1193 generalized concept, therefore, is obtained by substituting cells by nuclei as the sample entity.
 1194 This does not hold, however, for enucleated platelets.

1195 For studies of cells, we recommend that respiration be expressed, as far as possible, as:
 1196 (1) O_2 flux normalized for a mitochondrial marker, for separation of the effects of mitochondrial
 1197 quality and content on cell respiration (this includes *FCRs* as a normalization for a functional
 1198 mitochondrial marker); (2) O_2 flux in units of cell volume or mass, for comparison of respiration
 1199 of cells with different cell size (Renner *et al.* 2003) and with studies on tissue preparations, and
 1200 (3) O_2 flow in units of attomole (10^{-18} mol) of O_2 consumed in a second by each cell
 1201 [$\text{amol}\cdot\text{s}^{-1}\cdot\text{cell}^{-1}$], numerically equivalent to [$\text{pmol}\cdot\text{s}^{-1}\cdot 10^{-6}$ cells]. This convention allows
 1202 information to be easily used when designing experiments in which oxygen consumption must
 1203 be considered. For example, to estimate the volume-specific O_2 flux in an instrument chamber
 1204 that would be expected at a particular cell number concentration, one simply needs to multiply
 1205 the flow per cell by the number of cells per volume of interest. This provides the amount of O_2
 1206 [mol] consumed per time [s^{-1}] per unit volume [L^{-1}]. At an O_2 flow of $100 \text{ amol}\cdot\text{s}^{-1}\cdot\text{cell}^{-1}$ and a
 1207 cell density of $10^9 \text{ cells}\cdot\text{L}^{-1}$ ($10^6 \text{ cells}\cdot\text{mL}^{-1}$), the volume-specific O_2 flux is $100 \text{ nmol}\cdot\text{s}^{-1}\cdot\text{L}^{-1}$ (100
 1208 $\text{pmol}\cdot\text{s}^{-1}\cdot\text{mL}^{-1}$).

1209 ET-capacity in human cell types including HEK 293, primary HUVEC and fibroblasts
 1210 ranges from 50 to $180 \text{ amol}\cdot\text{s}^{-1}\cdot\text{cell}^{-1}$, measured in intact cells in the noncoupled state (see
 1211 Gnaiger 2014). At $100 \text{ amol}\cdot\text{s}^{-1}\cdot\text{cell}^{-1}$ corrected for *Rox*, the current across the mt-membranes,
 1212 $I_{e\text{H}^+}$, approximates $193 \text{ pA}\cdot\text{cell}^{-1}$ or 0.2 nA per cell. See Rich (2003) for an extension of
 1213 quantitative bioenergetics from the molecular to the human scale, with a transmembrane proton
 1214 flux equivalent to 520 A in an adult at a catabolic power of -110 W. Modelling approaches
 1215 illustrate the link between protonmotive force and currents (Willis *et al.* 2016).

1216 We consider isolated mitochondria as powerhouses and proton pumps as molecular
 1217 machines to relate experimental results to energy metabolism of the intact cell. The cellular
 1218 $\text{P}\gg/\text{O}_2$ based on oxidation of glycogen is increased by the glycolytic (fermentative) substrate-
 1219 level phosphorylation of 3 $\text{P}\gg/\text{Glyc}$ or 0.5 mol $\text{P}\gg$ for each mol O_2 consumed in the complete
 1220 oxidation of a mol glycosyl unit (Glyc). Adding 0.5 to the mitochondrial $\text{P}\gg/\text{O}_2$ ratio of 5.4
 1221 yields a bioenergetic cell physiological $\text{P}\gg/\text{O}_2$ ratio close to 6. Two NADH equivalents are
 1222 formed during glycolysis and transported from the cytosol into the mitochondrial matrix, either
 1223 by the malate-aspartate shuttle or by the glycerophosphate shuttle resulting in different
 1224 theoretical yields of ATP generated by mitochondria, the energetic cost of which potentially
 1225 must be taken into account. Considering also substrate-level phosphorylation in the TCA cycle,
 1226 this high $\text{P}\gg/\text{O}_2$ ratio not only reflects proton translocation and OXPHOS studied in isolation,
 1227 but integrates mitochondrial physiology with energy transformation in the living cell (Gnaiger
 1228 1993a).

1229
1230

1231 4. Conclusions

1232
1233
1234
1235

MitoEAGLE can serve as a gateway to better diagnose mitochondrial respiratory defects
 linked to genetic variation, age-related health risks, sex-specific mitochondrial performance,
 lifestyle with its effects on degenerative diseases, and thermal and chemical environment. The

1236 present recommendations on coupling control states and rates, linked to the concept of the
 1237 protonmotive force, are focused on studies with mitochondrial preparations. These will be
 1238 extended in a series of reports on pathway control of mitochondrial respiration, respiratory
 1239 states in intact cells, and harmonization of experimental procedures.

1240

1241 **Table 8. Terms, symbols, and units.**

1242 1243 1244 1245	Term	Symbol	SI unit	Links and comments
1246	alternative quinol oxidase	AOX		Fig. 1
1247	amount of substance B	n_B	[mol]	
1248	Complexes I to IV	CI to CIV		respiratory ET Complexes; Fig. 1
1249	concentration of substance B	$c_B = n_B \cdot V^{-1}$; [B]	[mol·m ⁻³]	Box 2
1250	electron transfer system	ETS		
1251	flow, for substance B	I_B	[mol·s ⁻¹]	system-related extensive quantity; Fig. 6
1252	flux, for substance B	J_B	<i>varies</i>	size-specific quantity; Fig. 6
1253	inorganic phosphate	P_i		
1254	LEAK	LEAK		Tab. 1
1255	mass of sample X	m_X	[kg]	Tab. 4
1256	mass of entity X	M_X	[kg]	Tab. 4
1257	MITOCARTA			https://www.broadinstitute.org/scientific-community/science/programs/metabolic-disease-program/publications/mitocarta/mitocarta-in-0
1258	MitoPedia			http://www.bioblast.at/index.php/MitoPedia
1259	mitochondria or mitochondrial	mt		Box 1
1260	mitochondrial DNA	mtDNA		Box 1
1261	mitochondrial concentration	$C_{mtE} = mtE \cdot V^{-1}$	[mtEU·m ⁻³]	Tab. 4
1262	mitochondrial content	$mtE_X = mtE \cdot N_X^{-1}$	[mtEU·x ⁻¹]	Tab. 4
1263	mitochondrial elemental unit	mtEU	<i>varies</i>	Tab. 4, specific units for mt-marker
1264	mitochondrial inner membrane	mtIM		MIM is widely used, and M is replaced by mt as abbreviation for mitochondria; Box 1
1265	mitochondrial outer membrane	mtOM		MOM is widely used, and M is replaced by mt as abbreviation for mitochondria; Box 1
1266	mitochondrial recovery	Y_{mtE}		
1267	mitochondrial yield	$Y_{mtE/m}$		$Y_{mtE/m} = Y_{mtE} \cdot D_{mtE}$
1268	negative	neg		Fig. 2
1269	number concentration of X	C_{NX}	[x·m ⁻³]	Tab. 4
1270	number of entities X	N_X	[x]	Tab. 4, Fig. 7
1271	number of entity B	N_B	[x]	Tab. 4
1272	oxidative phosphorylation	OXPPOS		Tab. 1
1273	oxygen concentration	$c_{O_2} = n_{O_2} \cdot V^{-1}$; [O ₂]	[mol·m ⁻³]	Section 3.2
1274	phosphorylation of ADP to ATP	P»		Section 2.2
1275	positive	pos		Fig. 2
1276	proton in the negative compartment	H ⁺ _{neg}		Fig. 2
1277	proton in the positive compartment	H ⁺ _{pos}		Fig. 2
1278	rate of electron transfer in ET state	E		ET-capacity; Tab. 1
1279	rate of LEAK respiration	L		Tab. 1
1280	rate of oxidative phosphorylation	P		OXPPOS capacity; Tab. 1
1281	rate of residual oxygen consumption	R_{ox}		Tab. 1
1282	residual oxygen consumption	ROX		Tab. 1
1283	specific mitochondrial density	$D_{mtE} = mtE \cdot m_X^{-1}$	[mtEU·kg ⁻¹]	Tab. 7
1284	volume	V	[m ³]	
1285	weight, dry weight	W_d	[kg]	used as mass of sample X; Fig. 6
1286	weight, wet weight	W_w	[kg]	used as mass of sample X; Fig. 6

1297 The optimal choice for expressing mitochondrial and cell respiration (**Box 3**) as O₂ flow
 1298 per biological system, and normalization for specific tissue-markers (volume, mass, protein)
 1299 and mitochondrial markers (volume, protein, content, mtDNA, activity of marker enzymes,
 1300 respiratory reference state) is guided by the scientific question under study. Interpretation of
 1301 the obtained data depends critically on appropriate normalization, and therefore reporting rates
 1302 merely as nmol·s⁻¹ is discouraged, since it restricts the analysis to intra-experimental
 1303 comparison of relative (qualitative) differences. Expressing O₂ consumption per cell may not
 1304 be possible when dealing with tissues. For studies with mitochondrial preparations, we
 1305 recommend that normalizations be provided as far as possible: (1) on a per cell basis as O₂ flow
 1306 (a biophysical normalization); (2) per g cell or tissue protein, or per cell or tissue mass as mass-
 1307 specific O₂ flux (a cellular normalization); and (3) per mitochondrial marker as mt-specific flux
 1308 (a mitochondrial normalization). With information on cell size and the use of multiple
 1309 normalizations, maximum potential information is available (Renner *et al.* 2003; Wagner *et al.*
 1310 2011; Gnaiger 2014).

1311 When using isolated mitochondria, total mitochondrial protein is a frequently applied
 1312 mitochondrial marker, the use of which is restricted to isolated mitochondria. The
 1313 mitochondrial recovery and yield, and experimental criteria for evaluation of purity versus
 1314 integrity should be reported. Mitochondrial markers—such as citrate synthase activity as an
 1315 enzymatic matrix marker—provide a link to the tissue of origin on the basis of calculating the
 1316 mitochondrial recovery, *i.e.*, the fraction of mitochondrial marker obtained from a unit mass of
 1317 tissue.

1318

1319 **Box 3: Mitochondrial and cell respiration**

1320

1321 Mitochondrial and cell respiration is the process of exergonic and exothermic energy
 1322 transformation in which scalar redox reactions are coupled to vectorial ion translocation across
 1323 a semipermeable membrane, which separates the small volume of a bacterial cell or
 1324 mitochondrion from the larger volume of its surroundings. The electrochemical exergy can be
 1325 partially conserved in the phosphorylation of ADP to ATP or in ion pumping, or dissipated in
 1326 an electrochemical short-circuit. Respiration is thus clearly distinguished from fermentation as
 1327 the counterpart of cellular core energy metabolism. Respiration is separated in mitochondrial
 1328 preparations from the partial contribution of fermentative pathways of the intact cell. Residual
 1329 oxygen consumption—as measured after inhibition of mitochondrial electron transfer—does
 1330 not belong to the class of catabolic reactions and is, therefore, subtracted from total oxygen
 1331 consumption to obtain baseline-corrected respiration.

1332

1333 Terms and symbols are summarized in **Table 8**. Their use will facilitate transdisciplinary
 1334 communication and support further developments towards a consistent theory of bioenergetics
 1335 and mitochondrial physiology. Technical terms related to and defined with normal words can
 1336 be used as index terms in databases, support the creation of ontologies towards semantic
 1337 information processing (MitoPedia), and help in communicating analytical findings as
 1338 impactful data-driven stories. *‘Making data available without making it understandable may be
 1339 worse than not making it available at all’* (National Academies of Sciences, Engineering, and
 1340 Medicine 2018). This is a call to carefully contribute to FAIR principles (Findable, Accessible,
 1341 Interoperable, Reusable) for the sharing of scientific data.

1342

1343 **Acknowledgements**

1344 We thank M. Beno for management assistance. Supported by COST Action CA15203
 1345 MitoEAGLE and K-Regio project MitoFit (E.G.).

1346

1347 **Competing financial interests:** E.G. is founder and CEO of Oroboros Instruments, Innsbruck,
1348 Austria.

1349

1350 5. References

1351

1352 Altmann R (1894) Die Elementarorganismen und ihre Beziehungen zu den Zellen. Zweite vermehrte Auflage.
1353 Verlag Von Veit & Comp, Leipzig:160 pp.

1354 Beard DA (2005) A biophysical model of the mitochondrial respiratory system and oxidative phosphorylation.
1355 PLoS Comput Biol 1(4):e36.

1356 Benda C (1898) Weitere Mitteilungen über die Mitochondria. Verh Dtsch Physiol Ges:376-83.

1357 Birkedal R, Laasmaa M, Vendelin M (2014) The location of energetic compartments affects energetic
1358 communication in cardiomyocytes. Front Physiol 5:376.

1359 Breton S, Beaupré HD, Stewart DT, Hoeh WR, Blier PU (2007) The unusual system of doubly uniparental
1360 inheritance of mtDNA: isn't one enough? Trends Genet 23:465-74.

1361 Brown GC (1992) Control of respiration and ATP synthesis in mammalian mitochondria and cells. Biochem J
1362 284:1-13.

1363 Calvo SE, Klauser CR, Mootha VK (2016) MitoCarta2.0: an updated inventory of mammalian mitochondrial
1364 proteins. Nucleic Acids Research 44:D1251-7.

1365 Calvo SE, Julien O, Clauser KR, Shen H, Kamer KJ, Wells JA, Mootha VK (2017) Comparative analysis of
1366 mitochondrial N-termini from mouse, human, and yeast. Mol Cell Proteomics 16:512-23.

1367 Campos JC, Queliconi BB, Bozi LHM, Bechara LRG, Dourado PMM, Andres AM, Jannig PR, Gomes KMS,
1368 Zambelli VO, Rocha-Resende C, Guatimosim S, Brum PC, Mochly-Rosen D, Gottlieb RA, Kowaltowski AJ,
1369 Ferreira JCB (2017) Exercise reestablishes autophagic flux and mitochondrial quality control in heart failure.
1370 Autophagy 13:1304-317.

1371 Canton M, Luvisetto S, Schmehl I, Azzone GF (1995) The nature of mitochondrial respiration and
1372 discrimination between membrane and pump properties. Biochem J 310:477-81.

1373 Chance B, Williams GR (1955a) Respiratory enzymes in oxidative phosphorylation. I. Kinetics of oxygen
1374 utilization. J Biol Chem 217:383-93.

1375 Chance B, Williams GR (1955b) Respiratory enzymes in oxidative phosphorylation: III. The steady state. J Biol
1376 Chem 217:409-27.

1377 Chance B, Williams GR (1955c) Respiratory enzymes in oxidative phosphorylation. IV. The respiratory chain. J
1378 Biol Chem 217:429-38.

1379 Chance B, Williams GR (1956) The respiratory chain and oxidative phosphorylation. Adv Enzymol Relat Subj
1380 Biochem 17:65-134.

1381 Cobb LJ, Lee C, Xiao J, Yen K, Wong RG, Nakamura HK, Mehta HH, Gao Q, Ashur C, Huffman DM, Wan J,
1382 Muzumdar R, Barzilai N, Cohen P (2016) Naturally occurring mitochondrial-derived peptides are age-
1383 dependent regulators of apoptosis, insulin sensitivity, and inflammatory markers. Aging (Albany NY) 8:796-
1384 809.

1385 Cohen ER, Cvitas T, Frey JG, Holmström B, Kuchitsu K, Marquardt R, Mills I, Pavese F, Quack M, Stohner J,
1386 Strauss HL, Takami M, Thor HL (2008) Quantities, units and symbols in physical chemistry, IUPAC Green
1387 Book, 3rd Edition, 2nd Printing, IUPAC & RSC Publishing, Cambridge.

1388 Cooper H, Hedges LV, Valentine JC, eds (2009) The handbook of research synthesis and meta-analysis. Russell
1389 Sage Foundation.

1390 Coopersmith J (2010) Energy, the subtle concept. The discovery of Feynman's blocks from Leibnitz to Einstein.
1391 Oxford University Press:400 pp.

1392 Cummins J (1998) Mitochondrial DNA in mammalian reproduction. Rev Reprod 3:172-82.

1393 Dai Q, Shah AA, Garde RV, Yonish BA, Zhang L, Medvitz NA, Miller SE, Hansen EL, Dunn CN, Price TM
1394 (2013) A truncated progesterone receptor (PR-M) localizes to the mitochondrion and controls cellular
1395 respiration. Mol Endocrinol 27:741-53.

1396 Divakaruni AS, Brand MD (2011) The regulation and physiology of mitochondrial proton leak. Physiology
1397 (Bethesda) 26:192-205.

1398 Doerrier C, Garcia-Souza LF, Krumschnabel G, Wohlfarter Y, Mészáros AT, Gnaiger E (2018) High-Resolution
1399 Fluorespirometry and OXPHOS protocols for human cells, permeabilized fibres from small biopsies of
1400 muscle and isolated mitochondria. Methods Mol. Biol. (in press)

1401 Doskey CM, van 't Erve TJ, Wagner BA, Buettner GR (2015) Moles of a substance per cell is a highly
1402 informative dosing metric in cell culture. PLOS ONE 10:e0132572.

1403 Drahotová Z, Milerová M, Stieglerová A, Houstek J, Ostádal B (2004) Developmental changes of cytochrome c
1404 oxidase and citrate synthase in rat heart homogenate. Physiol Res 53:119-22.

1405 Duarte FV, Palmeira CM, Rolo AP (2014) The role of microRNAs in mitochondria: small players acting wide.
1406 Genes (Basel) 5:865-86.

1407 Ernster L, Schatz G (1981) Mitochondria: a historical review. J Cell Biol 91:227s-55s.

- 1408 Estabrook RW (1967) Mitochondrial respiratory control and the polarographic measurement of ADP:O ratios.
1409 *Methods Enzymol* 10:41-7.
- 1410 Faber C, Zhu ZJ, Castellino S, Wagner DS, Brown RH, Peterson RA, Gates L, Barton J, Bickett M, Hagerty L,
1411 Kimbrough C, Sola M, Bailey D, Jordan H, Elangbam CS (2014) Cardiolipin profiles as a potential
1412 biomarker of mitochondrial health in diet-induced obese mice subjected to exercise, diet-restriction and
1413 ephedrine treatment. *J Appl Toxicol* 34:1122-9.
- 1414 Fell D (1997) Understanding the control of metabolism. Portland Press.
- 1415 Garlid KD, Beavis AD, Ratkje SK (1989) On the nature of ion leaks in energy-transducing membranes. *Biochim*
1416 *Biophys Acta* 976:109-20.
- 1417 Garlid KD, Semrad C, Zinchenko V. Does redox slip contribute significantly to mitochondrial respiration? In:
1418 Schuster S, Rigoulet M, Ouhabi R, Mazat J-P, eds (1993) *Modern trends in biothermokinetics*. Plenum Press,
1419 New York, London:287-93.
- 1420 Gerö D, Szabo C (2016) Glucocorticoids suppress mitochondrial oxidant production via upregulation of
1421 uncoupling protein 2 in hyperglycemic endothelial cells. *PLoS One* 11:e0154813.
- 1422 Gnaiger E. Efficiency and power strategies under hypoxia. Is low efficiency at high glycolytic ATP production a
1423 paradox? In: *Surviving Hypoxia: Mechanisms of Control and Adaptation*. Hochachka PW, Lutz PL, Sick T,
1424 Rosenthal M, Van den Thillart G, eds (1993a) CRC Press, Boca Raton, Ann Arbor, London, Tokyo:77-109.
- 1425 Gnaiger E (1993b) Nonequilibrium thermodynamics of energy transformations. *Pure Appl Chem* 65:1983-2002.
- 1426 Gnaiger E (2001) Bioenergetics at low oxygen: dependence of respiration and phosphorylation on oxygen and
1427 adenosine diphosphate supply. *Respir Physiol* 128:277-97.
- 1428 Gnaiger E (2009) Capacity of oxidative phosphorylation in human skeletal muscle. New perspectives of
1429 mitochondrial physiology. *Int J Biochem Cell Biol* 41:1837-45.
- 1430 Gnaiger E (2014) Mitochondrial pathways and respiratory control. An introduction to OXPHOS analysis. 4th ed.
1431 *Mitochondr Physiol Network* 19.12. Oroboros MiPNet Publications, Innsbruck:80 pp.
- 1432 Gnaiger E, Méndez G, Hand SC (2000) High phosphorylation efficiency and depression of uncoupled respiration
1433 in mitochondria under hypoxia. *Proc Natl Acad Sci USA* 97:11080-5.
- 1434 Greggio C, Jha P, Kulkarni SS, Lagarrigue S, Broskey NT, Boutant M, Wang X, Conde Alonso S, Ofori E,
1435 Auwerx J, Cantó C, Amati F (2017) Enhanced respiratory chain supercomplex formation in response to
1436 exercise in human skeletal muscle. *Cell Metab* 25:301-11.
- 1437 Hinkle PC (2005) P/O ratios of mitochondrial oxidative phosphorylation. *Biochim Biophys Acta* 1706:1-11.
- 1438 Hofstadter DR (1979) Gödel, Escher, Bach: An eternal golden braid. A metaphorical fugue on minds and
1439 machines in the spirit of Lewis Carroll. Harvester Press:499 pp.
- 1440 Illaste A, Laasmaa M, Peterson P, Vendelin M (2012) Analysis of molecular movement reveals latticelike
1441 obstructions to diffusion in heart muscle cells. *Biophys J* 102:739-48.
- 1442 Jasienski M, Bazzaz FA (1999) The fallacy of ratios and the testability of models in biology. *Oikos* 84:321-26.
- 1443 Jepihina N, Beraud N, Sepp M, Birkedal R, Vendelin M (2011) Permeabilized rat cardiomyocyte response
1444 demonstrates intracellular origin of diffusion obstacles. *Biophys J* 101:2112-21.
- 1445 Klepinin A, Ounpuu L, Guzun R, Chekulayev V, Timohhina N, Tepp K, Shevchuk I, Schlattner U, Kaambre T
1446 (2016) Simple oxygraphic analysis for the presence of adenylate kinase 1 and 2 in normal and tumor cells. *J*
1447 *Bioenerg Biomembr* 48:531-48.
- 1448 Klingenberg M (2017) UCP1 - A sophisticated energy valve. *Biochimie* 134:19-27.
- 1449 Koit A, Shevchuk I, Ounpuu L, Klepinin A, Chekulayev V, Timohhina N, Tepp K, Puurand M, Truu L, Heck K,
1450 Valvere V, Guzun R, Kaambre T (2017) Mitochondrial respiration in human colorectal and breast cancer
1451 clinical material is regulated differently. *Oxid Med Cell Longev* 1372640.
- 1452 Komlódi T, Tretter L (2017) Methylene blue stimulates substrate-level phosphorylation catalysed by succinyl-
1453 CoA ligase in the citric acid cycle. *Neuropharmacology* 123:287-98.
- 1454 Lane N (2005) Power, sex, suicide: mitochondria and the meaning of life. Oxford University Press:354 pp.
- 1455 Larsen S, Nielsen J, Neigaard Nielsen C, Nielsen LB, Wibrand F, Stride N, Schroder HD, Boushel RC, Helge
1456 JW, Dela F, Hey-Mogensen M (2012) Biomarkers of mitochondrial content in skeletal muscle of healthy
1457 young human subjects. *J Physiol* 590:3349-60.
- 1458 Lee C, Zeng J, Drew BG, Sallam T, Martin-Montalvo A, Wan J, Kim SJ, Mehta H, Hevener AL, de Cabo R,
1459 Cohen P (2015) The mitochondrial-derived peptide MOTS-c promotes metabolic homeostasis and reduces
1460 obesity and insulin resistance. *Cell Metab* 21:443-54.
- 1461 Lee SR, Kim HK, Song IS, Youm J, Dizon LA, Jeong SH, Ko TH, Heo HJ, Ko KS, Rhee BD, Kim N, Han J
1462 (2013) Glucocorticoids and their receptors: insights into specific roles in mitochondria. *Prog Biophys Mol*
1463 *Biol* 112:44-54.
- 1464 Leek BT, Mudaliar SR, Henry R, Mathieu-Costello O, Richardson RS (2001) Effect of acute exercise on citrate
1465 synthase activity in untrained and trained human skeletal muscle. *Am J Physiol Regul Integr Comp Physiol*
1466 280:R441-7.
- 1467 Lemieux H, Blier PU, Gnaiger E (2017) Remodeling pathway control of mitochondrial respiratory capacity by
1468 temperature in mouse heart: electron flow through the Q-junction in permeabilized fibers. *Sci Rep* 7:2840.

- 1469 Lenaz G, Tioli G, Falasca AI, Genova ML (2017) Respiratory supercomplexes in mitochondria. In: Mechanisms
1470 of primary energy trasduction in biology. M Wikstrom (ed) Royal Society of Chemistry Publishing, London,
1471 UK:296-337.
- 1472 Margulis L (1970) Origin of eukaryotic cells. New Haven: Yale University Press.
- 1473 Meinild Lundby AK, Jacobs RA, Gehrig S, de Leur J, Hauser M, Bonne TC, Flück D, Dandanell S, Kirk N,
1474 Kaech A, Ziegler U, Larsen S, Lundby C (2018) Exercise training increases skeletal muscle mitochondrial
1475 volume density by enlargement of existing mitochondria and not de novo biogenesis. *Acta Physiol* 222,
1476 e12905.
- 1477 Menshikova EV, Ritov VB, Fairfull L, Ferrell RE, Kelley DE, Goodpaster BH (2006) Effects of exercise on
1478 mitochondrial content and function in aging human skeletal muscle. *J Gerontol A Biol Sci Med Sci* 61:534-
1479 40.
- 1480 Menshikova EV, Ritov VB, Ferrell RE, Azuma K, Goodpaster BH, Kelley DE (2007) Characteristics of skeletal
1481 muscle mitochondrial biogenesis induced by moderate-intensity exercise and weight loss in obesity. *J Appl*
1482 *Physiol* (1985) 103:21-7.
- 1483 Menshikova EV, Ritov VB, Toledo FG, Ferrell RE, Goodpaster BH, Kelley DE (2005) Effects of weight loss
1484 and physical activity on skeletal muscle mitochondrial function in obesity. *Am J Physiol Endocrinol Metab*
1485 288:E818-25.
- 1486 Miller GA (1991) The science of words. Scientific American Library New York:276 pp.
- 1487 Mitchell P (1961) Coupling of phosphorylation to electron and hydrogen transfer by a chemi-osmotic type of
1488 mechanism. *Nature* 191:144-8.
- 1489 Mitchell P (2011) Chemiosmotic coupling in oxidative and photosynthetic phosphorylation. *Biochim Biophys*
1490 *Acta Bioenergetics* 1807:1507-38.
- 1491 Mogensen M, Sahlin K, Fernström M, Glintborg D, Vind BF, Beck-Nielsen H, Højlund K (2007) Mitochondrial
1492 respiration is decreased in skeletal muscle of patients with type 2 diabetes. *Diabetes* 56:1592-9.
- 1493 Mohr PJ, Phillips WD (2015) Dimensionless units in the SI. *Metrologia* 52:40-7.
- 1494 Moreno M, Giacco A, Di Munno C, Goglia F (2017) Direct and rapid effects of 3,5-diiodo-L-thyronine (T2).
1495 *Mol Cell Endocrinol* 7207:30092-8.
- 1496 Morrow RM, Picard M, Derbeneva O, Leipzig J, McManus MJ, Gousspillou G, Barbat-Artigas S, Dos Santos C,
1497 Hepple RT, Murdock DG, Wallace DC (2017) Mitochondrial energy deficiency leads to hyperproliferation of
1498 skeletal muscle mitochondria and enhanced insulin sensitivity. *Proc Natl Acad Sci U S A* 114:2705-10.
- 1499 Murley A, Nunnari J (2016) The emerging network of mitochondria-organelle contacts. *Mol Cell* 61:648-53.
- 1500 National Academies of Sciences, Engineering, and Medicine (2018) International coordination for science data
1501 infrastructure: Proceedings of a workshop—in brief. Washington, DC: The National Academies Press. doi:
1502 <https://doi.org/10.17226/25015>.
- 1503 Paradies G, Paradies V, De Benedictis V, Ruggiero FM, Petrosillo G (2014) Functional role of cardiolipin in
1504 mitochondrial bioenergetics. *Biochim Biophys Acta* 1837:408-17.
- 1505 Pesta D, Gnaiger E (2012) High-Resolution Respirometry. OXPHOS protocols for human cells and
1506 permeabilized fibres from small biopsies of human muscle. *Methods Mol Biol* 810:25-58.
- 1507 Pesta D, Hoppel F, Macek C, Messner H, Faulhaber M, Kobel C, Parson W, Burtscher M, Schocke M, Gnaiger
1508 E (2011) Similar qualitative and quantitative changes of mitochondrial respiration following strength and
1509 endurance training in normoxia and hypoxia in sedentary humans. *Am J Physiol Regul Integr Comp Physiol*
1510 301:R1078–87.
- 1511 Price TM, Dai Q (2015) The role of a mitochondrial progesterone receptor (PR-M) in progesterone action.
1512 *Semin Reprod Med* 33:185-94.
- 1513 Puchowicz MA, Varnes ME, Cohen BH, Friedman NR, Kerr DS, Hoppel CL (2004) Oxidative phosphorylation
1514 analysis: assessing the integrated functional activity of human skeletal muscle mitochondria – case studies.
1515 *Mitochondrion* 4:377-85. Puntschart A, Claassen H, Jostarndt K, Hoppeler H, Billeter R (1995) mRNAs of
1516 enzymes involved in energy metabolism and mtDNA are increased in endurance-trained athletes. *Am J*
1517 *Physiol* 269:C619-25.
- 1518 Quiros PM, Mottis A, Auwerx J (2016) Mitonuclear communication in homeostasis and stress. *Nat Rev Mol*
1519 *Cell Biol* 17:213-26.
- 1520 Reichmann H, Hoppeler H, Mathieu-Costello O, von Bergen F, Pette D (1985) Biochemical and ultrastructural
1521 changes of skeletal muscle mitochondria after chronic electrical stimulation in rabbits. *Pflugers Arch* 404:1-
1522 9.
- 1523 Renner K, Amberger A, Konwalinka G, Gnaiger E (2003) Changes of mitochondrial respiration, mitochondrial
1524 content and cell size after induction of apoptosis in leukemia cells. *Biochim Biophys Acta* 1642:115-23.
- 1525 Rich P (2003) Chemiosmotic coupling: The cost of living. *Nature* 421:583.
- 1526 Rostovtseva TK, Sheldon KL, Hassanzadeh E, Monge C, Saks V, Bezrukov SM, Sackett DL (2008) Tubulin
1527 binding blocks mitochondrial voltage-dependent anion channel and regulates respiration. *Proc Natl Acad Sci*
1528 *USA* 105:18746-51.

- 1529 Rustin P, Parfait B, Chretien D, Bourgeron T, Djouadi F, Bastin J, Rötig A, Munnich A (1996) Fluxes of
1530 nicotinamide adenine dinucleotides through mitochondrial membranes in human cultured cells. *J Biol Chem*
1531 271:14785-90.
- 1532 Saks VA, Veksler VI, Kuznetsov AV, Kay L, Sikk P, Tiivel T, Tranqui L, Olivares J, Winkler K, Wiedemann F,
1533 Kunz WS (1998) Permeabilised cell and skinned fiber techniques in studies of mitochondrial function in
1534 vivo. *Mol Cell Biochem* 184:81-100.
- 1535 Salabei JK, Gibb AA, Hill BG (2014) Comprehensive measurement of respiratory activity in permeabilized cells
1536 using extracellular flux analysis. *Nat Protoc* 9:421-38.
- 1537 Sazanov LA (2015) A giant molecular proton pump: structure and mechanism of respiratory complex I. *Nat Rev*
1538 *Mol Cell Biol* 16:375-88.
- 1539 Schneider TD (2006) Claude Shannon: biologist. The founder of information theory used biology to formulate
1540 the channel capacity. *IEEE Eng Med Biol Mag* 25:30-3.
- 1541 Schönfeld P, Dymkowska D, Wojtczak L (2009) Acyl-CoA-induced generation of reactive oxygen species in
1542 mitochondrial preparations is due to the presence of peroxisomes. *Free Radic Biol Med* 47:503-9.
- 1543 Schultz J, Wiesner RJ (2000) Proliferation of mitochondria in chronically stimulated rabbit skeletal muscle--
1544 transcription of mitochondrial genes and copy number of mitochondrial DNA. *J Bioenerg Biomembr* 32:627-
1545 34.
- 1546 Simson P, Jepihhina N, Laasmaa M, Peterson P, Birkedal R, Vendelin M (2016) Restricted ADP movement in
1547 cardiomyocytes: Cytosolic diffusion obstacles are complemented with a small number of open mitochondrial
1548 voltage-dependent anion channels. *J Mol Cell Cardiol* 97:197-203.
- 1549 Stucki JW, Ineichen EA (1974) Energy dissipation by calcium recycling and the efficiency of calcium transport
1550 in rat-liver mitochondria. *Eur J Biochem* 48:365-75.
- 1551 Tonkonogi M, Harris B, Sahlin K (1997) Increased activity of citrate synthase in human skeletal muscle after a
1552 single bout of prolonged exercise. *Acta Physiol Scand* 161:435-6.
- 1553 Waczulikova I, Habodaszova D, Cagalinec M, Ferko M, Ulicna O, Mateasik A, Sikurova L, Ziegelhöffer A
1554 (2007) Mitochondrial membrane fluidity, potential, and calcium transients in the myocardium from acute
1555 diabetic rats. *Can J Physiol Pharmacol* 85:372-81.
- 1556 Wagner BA, Venkataraman S, Buettner GR (2011) The rate of oxygen utilization by cells. *Free Radic Biol Med*
1557 51:700-712.
- 1558 Wang H, Hiatt WR, Barstow TJ, Brass EP (1999) Relationships between muscle mitochondrial DNA content,
1559 mitochondrial enzyme activity and oxidative capacity in man: alterations with disease. *Eur J Appl Physiol*
1560 *Occup Physiol* 80:22-7.
- 1561 Watt IN, Montgomery MG, Runswick MJ, Leslie AG, Walker JE (2010) Bioenergetic cost of making an
1562 adenosine triphosphate molecule in animal mitochondria. *Proc Natl Acad Sci U S A* 107:16823-7.
- 1563 Weibel ER, Hoppeler H (2005) Exercise-induced maximal metabolic rate scales with muscle aerobic capacity. *J*
1564 *Exp Biol* 208:1635-44.
- 1565 White DJ, Wolff JN, Pierson M, Gemmell NJ (2008) Revealing the hidden complexities of mtDNA inheritance.
1566 *Mol Ecol* 17:4925-42.
- 1567 Wikström M, Hummer G (2012) Stoichiometry of proton translocation by respiratory complex I and its
1568 mechanistic implications. *Proc Natl Acad Sci U S A* 109:4431-6.
- 1569 Willis WT, Jackman MR, Messer JI, Kuzmiak-Glancy S, Glancy B (2016) A simple hydraulic analog model of
1570 oxidative phosphorylation. *Med Sci Sports Exerc* 48:990-1000.